

Dynamics and Stability of Non-Smooth Dynamical Systems with Two Switches

Guilherme Tavares da Silva  · Ricardo Miranda Martins 

Received: date / Accepted: date

Abstract One of the most common hypotheses on the theory of non-smooth dynamical systems is a regular surface as switching manifold, at which case there is at least well-defined and established Filippov dynamics. However, systems with singular switching manifolds still lack such well-established dynamics, although present in many relevant models of phenomena where multiple switches or multiple abrupt changes occur. At this work, we leverage a methodology that, through blow-ups and singular perturbation, allows the extension of Filippov dynamics to the singular case. Specifically, tridimensional systems whose switching manifold consists of an algebraic manifold with transversal self-intersection are considered. This configuration, known as double discontinuity, represents systems with two switches and whose singular part consists of a straight line, where ordinary Filippov dynamics is not directly applicable. For the general, non-linear case, beyond defining the so-called fundamental dynamics over the singular part, general theorems on its qualitative behavior are provided. For the affine case, however, theorems fully describing the fundamental dynamics are obtained. Finally, this fine-grained control over the dynamics is leveraged to derive Peixoto-like theorems characterizing semi-local structural stability.

Keywords Dynamical systems · Filippov systems · Singular perturbations (Mathematics) · Structural stability

G. T. da Silva · R. M. Martins (✉)
Departamento de Matemática, Universidade Estadual de Campinas,
Rua Sérgio Buarque de Holanda 651, Cidade Universitária Zeferino
Vaz, Campinas, SP, CEP 13083-859, Brazil
E-mail: rmiranda@unicamp.br

G. T. da Silva
E-mail: g119509@dac.unicamp.br

1 Introduction

The theory of dynamical systems given by ordinary differential equations

$$\dot{\mathbf{x}} = \mathbf{F}(\mathbf{x}), \quad (1)$$

where $\mathbf{F} : \mathbb{R}^n \rightarrow \mathbb{R}^n$ is at least a continuous vector field evolved naturally with the birth of Calculus itself, with [2] and [30] being exceptional modern references on the subject. In fact, the machinery provided by this theory has been used in the study of models all around science: from classical Newtonian Mechanics to modern Machine Learning [49].

However, either naturally or due to simplifications and practicality, many of these phenomena are better approached with non-smooth models, i.e., where the vector field \mathbf{F} above has discontinuities. More specifically, given $U \subset \mathbb{R}^n$ open, $h : U \rightarrow \mathbb{R}$ continually differentiable having 0 as a **regular value** and two vector fields $\mathbf{F}_{\pm} : U \rightarrow \mathbb{R}^n$ of class $C^k(U)$ with $k \geq 1$, we understand as a **non-smooth dynamical system** that given by a differential equation as (1) where

$$\mathbf{F}(\mathbf{x}) = \begin{cases} \mathbf{F}_+(\mathbf{x}), & \text{if } \mathbf{x} \in \Sigma_+, \\ \mathbf{F}_-(\mathbf{x}), & \text{if } \mathbf{x} \in \Sigma_-, \end{cases} \quad (2)$$

with $\Sigma_+ = \{\mathbf{x} \in U; h(\mathbf{x}) \geq 0\}$ and $\Sigma_- = \{\mathbf{x} \in U; h(\mathbf{x}) \leq 0\}$ intersecting at a regular surface Σ called **switching manifold**. We denote the set of vector fields \mathbf{F} defined as above by

$$\mathcal{R}^k(U) \equiv C^k(U, \mathbb{R}^n) \times C^k(U, \mathbb{R}^n)$$

which we consider equipped with the Whitney topology. Generally, we write $\mathbf{F} = (\mathbf{F}_+, \mathbf{F}_-)$ to denote the elements of this set. These systems arise frequently, for instance, in the study of mechanical systems with impact or friction [6,25,31,

50], electronic circuits with switches [4, 5, 10, 47], biological and climate models with abrupt changes [3, 9, 32, 37, 38], economics and politics [1, 45, 46], etc. Hence, not only due to its applications, but also, its mathematical beauty, the theory of non-smooth dynamical system is a very active field, attracting and mobilizing scientists from all around the world.

In this endeavor, the establishment of definitions is one of the main challenges. The definition of solution for a non-smooth system, for instance, is not always clear. Nevertheless, in this context, one of the greatest contributions came from Filippov in [20], which introduced a convention to define such solutions in such a way that, apparently, is both geometrically beautiful and consistent with the physical world¹. More specifically, for points $\mathbf{x} \in U \setminus \Sigma$, the usual local dynamics of the fields \mathbf{F}_\pm is considered. On the other hand, roughly speaking, for points $\mathbf{x} \in \Sigma$ and considering the Lie derivative $\mathbf{F}_\pm h(\mathbf{x}) := \nabla h(\mathbf{x}) \cdot \mathbf{F}_\pm(\mathbf{x})$, the switching manifold Σ splits into three regions:

– **Crossing Region:**

$\Sigma^{cr} = \{\mathbf{x} \in \Sigma; \mathbf{F}_+ h(\mathbf{x}) \mathbf{F}_- h(\mathbf{x}) > 0\}$, where touching trajectories cross Σ through concatenation.

– **Sliding Region:**

$\Sigma^{sl} = \{\mathbf{x} \in \Sigma; \mathbf{F}_+ h(\mathbf{x}) > 0, \mathbf{F}_- h(\mathbf{x}) < 0\}$, where touching trajectories remains tangent to Σ for positive time.

– **Escaping Region:**

$\Sigma^{es} = \{\mathbf{x} \in \Sigma; \mathbf{F}_+ h(\mathbf{x}) < 0, \mathbf{F}_- h(\mathbf{x}) > 0\}$, where touching trajectories remains tangent to Σ for negative time.

Due to the continuity, all regions above are open sets separated by the so-called **tangency points** $\mathbf{x} \in \Sigma$ where $\mathbf{F}_+ h(\mathbf{x}) \mathbf{F}_- h(\mathbf{x}) = 0$ which, dynamically, acts as singularities. Moreover, for points $\mathbf{x} \in \Sigma^s := \Sigma^{sl} \cup \Sigma^{es}$, the trajectory slides tangent to Σ according to a well-defined **sliding vector field** $\mathbf{F}^s : \Sigma^s \rightarrow T\Sigma^s$ given by

$$\mathbf{F}^s(\mathbf{x}) = \frac{\mathbf{F}_- h(\mathbf{x}) \mathbf{F}_+(\mathbf{x}) - \mathbf{F}_+ h(\mathbf{x}) \mathbf{F}_-(\mathbf{x})}{\mathbf{F}_- h(\mathbf{x}) - \mathbf{F}_+ h(\mathbf{x})}, \quad (3)$$

which consists of the single vector in the intersection

$$\text{Conv}(\{\mathbf{F}_+(\mathbf{x}), \mathbf{F}_-(\mathbf{x})\}) \cap \Sigma,$$

where $\text{Conv}(\cdot)$ represents **convex hull**.

Using the above construction, many advances have been achieved on this class of systems concerning, for instance, its bifurcations [23], regularization [36, 40, 43], structural stability [7, 22, 42] and uncountable works regarding minimal sets. However, as previously observed, the theory established by Filippov's convention has a fundamental hypothesis: a

regular surface as switching manifold between the smooth parts of the system, i.e., a surface $\Sigma = h^{-1}(\{0\})$ where 0 is a regular value of h . Many relevant phenomena, however, require a model where Σ is, actually, the preimage of a singular value. Generally speaking, models where two or more abrupt changes might occur. See, for instance, the ‘‘On or Off Genes’’ section in [28, p. 28], where a model is presented for two genes interacting in an organic cell of a living system in order to produce proteins. At that same reference, [28, p. 30], the section ‘‘Jittery Investments’’ presents another interesting model for a game with two players buying or selling stocks of a company.

In this context, an important class of non-smooth dynamical systems in \mathbb{R}^3 with singular switching manifold, known as Gutierrez-Sotomayor and described in [24], is obtained when the regularity condition is broken in a dynamically stable manner. More precisely, in order to avoid non-trivial recurrence on non-orientable manifolds, a restriction to Σ is imposed so that its smooth parts are either orientable or diffeomorphic to an open set of \mathbb{P}^2 (projective plane), \mathbb{K}^2 (Klein's bottle) or $G^2 = \mathbb{T}^2 \# \mathbb{P}^2$ (torus with cross-cap). After a proper coordinates normalization, this restriction leads to five algebraic manifolds, with a regular configuration

$$\mathcal{R} = \{(x, y, z) \in \mathbb{R}^3; z = 0\} \quad (4)$$

known as **regular discontinuity** and four singular configurations given by

$$\begin{aligned} \mathcal{D} &= \{(x, y, z) \in \mathbb{R}^3; xy = 0\}, \\ \mathcal{T} &= \{(x, y, z) \in \mathbb{R}^3; xyz = 0\}, \\ \mathcal{C} &= \{(x, y, z) \in \mathbb{R}^3; z^2 - x^2 - y^2 = 0\}, \\ \mathcal{W} &= \{(x, y, z) \in \mathbb{R}^3; zx^2 - y^2 = 0\}, \end{aligned} \quad (5)$$

and known as **double**, **triple**, **cone** and **Whitney discontinuities**, respectively. See Figure 1.

For systems whose switching manifold is homeomorphic to (4), the Filippov dynamics described above is fully applicable. In fact, these systems exactly corresponds to those described at the beginning of this text. However, for systems whose switching manifold is homeomorphic to one of the singular configurations (5), Filippov dynamics is not directly applicable to the whole manifold Σ . More precisely, the switching manifold can be decomposed in the following disjoint union:

$$\Sigma = \Sigma_{\mathcal{R}} \cup \Sigma_{\mathcal{S}} \quad (6)$$

where $\Sigma_{\mathcal{R}}$ consists, locally, of regular discontinuities; and $\Sigma_{\mathcal{S}}$ consists of points where Σ self-intersects, difficulting direct application of the usual Filippov dynamics. In fact,

¹ It is important to remark, however, that other conventions exist with equal beauty. Filippov's convention just happens to be the most accepted one nowadays. For instance, we cite here Carathéodory [41] and Utkin [44] conventions. See also [21] for some historical aspects.

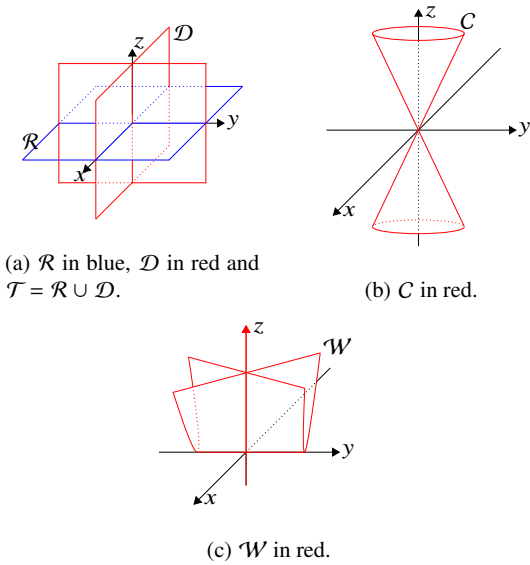


Fig. 1: Gutierrez-Sotomayor algebraic manifolds.

an attempt to directly generalize the Filippov convention to points in Σ_S , leads to the existence of up to infinite possible sliding fields, as proved at Lemma 2.4 of [26, p. 1087]. See Figure 2a.

In other words, the class of non-smooth dynamical systems $\mathbf{F} = (\mathbf{F}_i)$ whose switching manifold is homeomorphic to one of those at (5), in the sense of Gutierrez-Sotomayor, represents the simplest singular systems. However, besides its many applications, knowledge of its dynamics is scarce. In particular, over the last decade, three main methodologies arose to study these systems. Not necessarily in chronological order, these methodologies are briefly presented below.

The first one, presented in [26] by Jeffrey, propose an extension of the Filippov dynamics to Σ_S through the so-called “canopy”, a convex-like ruled surface, built with the convex hull $\text{Conv}(\{\mathbf{F}_i\})$, which can be proved to intersect Σ at a finite number of points, see Figure 2b. Each one of these intersections represents a sliding vector and, therefore, this methodology leads again to non-uniqueness of the sliding field. To deal with this lack of uniqueness, the author there conjectures the so-called “dummy dynamics” acting over the canopy. This idea led to many results such as, for instance, [27, 29, 48]. However, as stated at [26, p. 1102], a justification for the dummy dynamics remains an open problem.

The next one, presented in [17] by Dieci *et al.*, although older than the previous methodology, proposes a similar construction where, again, non-uniqueness of sliding vectors happens. Here, however, the authors show that, imposing certain attractivity hypothesis on the switching manifold Σ , many conclusions can be proved on the behavior of the dynamics. In fact, this idea led to the sequence of works [11–16, 18] where several aspects of the dynamics are

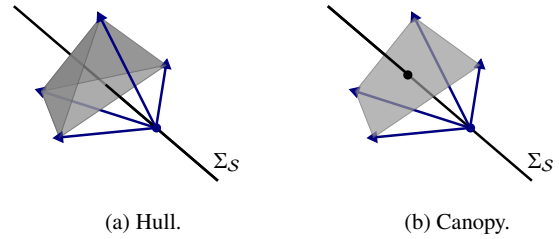


Fig. 2: Convex hull and canopy.

explored under different types of attractivity: from minimal sets to structural stability. However, imposing conditions on Σ is a fundamental and restrictive hypothesis here.

Finally, [8] by Buzzi *et al.*, propose an extension of the Filippov dynamics to Σ_S through the application of a proper blow-up and use of Geometrical Singular Perturbation Theory (see [19, 43]), or GSP-Theory for short, to study the resulting slow-fast systems. Although distant from a direct generalization of Filippov’s convention, this methodology is also a natural approach with advantages over the previous ones. In fact, while the non-uniqueness of the sliding field is also predicted, here it is managed naturally, as will be seen over the text. Moreover, yet in comparison with the previous ones, due to the blow-up, this methodology provides a broader view of the dynamics – appropriate for the codimension of the problem. Even more, no assumptions neither on Σ or the underlying vector fields \mathbf{F}_i are required here. However, both [8] and the posterior works [33, 36, 43] lack a clear presentation and justification for the dynamics induced over Σ_S . Up to our knowledge, there are no works focused on the study of this dynamics for any class of fields \mathbf{F}_i such as, for instance, linear ones. In fact, the main focus of the above-cited works lies on the verification that, after the blow-up, the resulting system contains only regular discontinuities or, in other words, Theorem 4.1 with some sparse examples lacking proper justification for the underlying dynamics: see, for instance, the examples in [8, p. 449], [43, p. 1952], and the remark and example in [33, p. 501].

Given the arguments above, for this text, we embrace and leverage Buzzi’s blow-up based methodology to study the dynamics associated with singular switching manifolds, since it

1. does not depend on imposing conditions on Σ ;
2. deals naturally with the non-uniqueness of sliding vectors; and
3. provide a broader view of the dynamics over Σ_S .

Specifically, we deal essentially with the Gutierrez-Sotomayor algebraic manifold \mathcal{D} , the double discontinuity, both an equivalent in \mathbb{R}^2 and the traditional in \mathbb{R}^3 , whose classes of vector fields are henceforth denoted \mathcal{D}_2^k and \mathcal{D}_3^k , respectively, see Figure 3. Geometrically, these configurations rep-

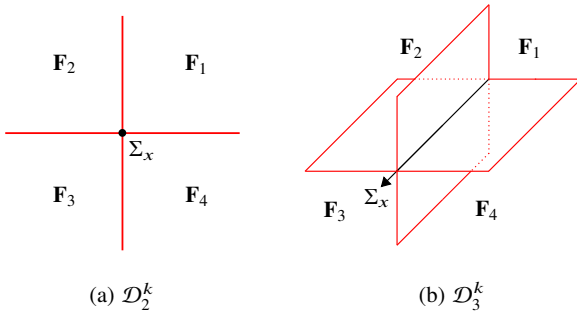


Fig. 3: Double discontinuity.

resent transversal self-intersections of the switching manifold. After a general qualitative study on the non-linear case, we focus on systems given by affine vector fields

$$\mathbf{F}_i(\mathbf{x}) = \mathbf{A}_i \mathbf{x} + \mathbf{b}_i,$$

where \mathbf{A}_i and \mathbf{b}_i are real matrices for every $i \in \{1, 2, 3, 4\}$ respectively of sizes $j \times j$ and $j \times 1$, with $j \in \{2, 3\}$ representing the dimension and progressively increasing its complexity: starting at the constant case ($\mathbf{A}_i = \mathbf{0}$), linear ($\mathbf{b}_i = \mathbf{0}$) and then, finally, the complete affine case. We denote these classes of constant, linear and affine vector fields, respectively, as \mathcal{C}_j , \mathcal{L}_j and \mathcal{A}_j . This program assures a progressive and effective increase on the intuition and understanding of the dynamics.

For the class \mathcal{D}_3^k of piecewise vector fields having the traditional Double Discontinuity as switching manifold, see Figure 3b, we tackle the main problem of defining a dynamics over Σ_S , here given by a straight line Σ_x . In particular, we use the cylindrical blow-up suggested in [33] to induce a dynamics over Σ_x , with GSP-Theory playing a major role. As a result, we obtain the **Fundamental Lemma 4.1** stated below, which improves *Buzzi's* methodology by clarifying the issues raised above:

Lemma 4.1 (Fundamental Dynamics) *Given $\mathbf{F} \in \mathcal{D}_3^k$ with components $\mathbf{F}_i = (w_i, p_i, q_i)$, let $\tilde{\mathbf{F}} \in \tilde{\mathcal{D}}_3^k$ be the vector field induced by the blow-up*

$$\phi_1(x, \theta, r) = (x, r \cos \theta, r \sin \theta).$$

Then, this blow-up associates the dynamics over Σ_x with the following dynamics over the cylinder $C = \mathbb{R} \times S^1 = S_1 \cup \dots \cup S_4$: over each stripe S_i acts a slow-fast dynamics whose reduced dynamics is given by

$$\begin{cases} \dot{x} = w_i \\ 0 = q_i \cos \theta - p_i \sin \theta \end{cases} \quad (24)$$

with slow radial dynamics $\dot{r} = p_i \cos \theta + q_i \sin \theta$; and layer dynamics given by

$$\begin{cases} x' = 0 \\ \theta' = q_i \cos \theta - p_i \sin \theta \end{cases} \quad (25)$$

with fast radial dynamics $r' = 0$. Finally, at every equation above the functions w_i , p_i and q_i must be calculated at the point $\phi_1(x, \theta, 0) = (x, 0, 0)$.

We note here that no blowing-down is ever carried out over this text, i.e., once we have the blow-up induced (fundamental) dynamics above over the cylinder C , the inverse operation is never performed to recover a dynamics over Σ_x with the original coordinates. Actually, this operation would make little to no sense most of the times given the higher codimension of Σ_x , i.e., most of the information on the dynamics would be lost. For instance, under the so-called **fundamental hypothesis** (WFH) or (SFH), the fundamental lemma assures not only the sequence of qualitative theorems bellow for the general, non-linear case, but also most of the original results in this text and, hence, its name.

Theorem 4.2 *The radial dynamics can only be transversal ($\dot{r} \neq 0$) to the cylinder C over the slow manifold \mathcal{M}_i . More over, under (WFH), it is in fact transversal.*

Theorem 4.3 *The slow manifold \mathcal{M}_i is locally a graph $(x, \theta(x))$ under (WFH). However, if $\|(f_i)_\theta\|$ admits a global positive minimum, then \mathcal{M}_i is globally a graph $(x, \theta(x))$. Either way, $\theta(x)$ is of class C^k .*

Theorem 4.4 *The slow manifold \mathcal{M}_i is normally hyperbolic at every point that satisfies (WFH).*

Theorem 4.5 *The hyperbolic singularities of the reduced system (24) acts as hyperbolic saddle or node singularities of S_i under (WFH).*

Then, using these fundamental dynamics, we focus on the constant (\mathcal{C}_3) and affine (\mathcal{A}_3) cases, to fully describe the respective induced dynamics over the cylinder as stated in Theorem 5.1 for the constant case and Theorem 6.1 below for the affine case.

Theorem 6.1 (Affine Dynamics) *Given $\mathbf{F} \in \mathcal{A}_3$ with affine components \mathbf{F}_i given by (31) and such that $\gamma_i \neq 0$, let $\tilde{\mathbf{F}} \in \tilde{\mathcal{A}}_3$ be the vector field induced by the blow-up $\phi_1(x, \theta, r) = (x, r \cos \theta, r \sin \theta)$. Then, this blow-up associates the dynamics over Σ_x with the following fundamental dynamics over the cylinder $C = \mathbb{R} \times S^1 = S_1 \cup \dots \cup S_4$: over each stripe S_i acts a slow-fast dynamics whose slow manifold is given by $\mathcal{M}_i = A_i \cup A_i^\pi$, where A_i^π is a π -translation of A_i in θ*

1. case $a_{i2} \neq 0$, then

$$A_i = \{(x, \theta) \in [-\infty, \alpha_i] \times [0, 2\pi]; \theta = \theta_i(x) + \pi\} \cup \\ \cup \{(x, \theta) \in [\alpha_i, +\infty] \times [0, 2\pi]; \theta = \theta_i(x)\}$$

with $\theta_i(x) = \arctan\left(\frac{a_{i3}x+d_{i3}}{a_{i2}x+d_{i2}}\right)$, which consists of an arc-tangent-like curve inside the cylinder C with $\theta = \beta_i + \pi$ and $\theta = \beta_i$ as negative and positive horizontal asymptotes, respectively;

2. case $a_{i2} = 0$, then

$$A_i = \{(x, \theta) \in \mathbb{R} \times [0, 2\pi]; \theta = \theta_i(x)\}$$

with $\theta_i(x) = \arctan\left(\frac{a_{i3}x+d_{i3}}{d_{i2}}\right)$, which consists of an arc-tangent-like curve inside the cylinder C with $\theta = \sigma_{i-}$ and $\theta = \sigma_{i+}$ as negative and positive horizontal asymptotes, respectively.

Both arctangents are increasing if $\gamma_i > 0$ and decreasing if $\gamma_i < 0$. Over them act the reduced dynamics $\dot{x} = a_{i1}x + d_{i1}$ and, around them, acts the layer dynamics described in Table 3, but exchanging a_{i2} with d_{i2} if $a_{i2} = 0$. Finally, the new parameters above are given by $\alpha_i = -\frac{d_{i2}}{a_{i2}}$, $\beta_i = \arctan\left(\frac{a_{i3}}{a_{i2}}\right)$, $\gamma_i = a_{i3}d_{i2} - d_{i3}a_{i2}$, $\delta_i = -\frac{d_{i1}}{a_{i1}}$ and $\sigma_{i\pm} = \pm \operatorname{sgn}(\gamma_i)\frac{\pi}{2}$.

Finally, combining this fine-grained control of the fundamental dynamics with the structural stability characterization provided by [7], we also derive Peixoto-like theorems characterizing semi-local structural stability of the dynamics over the cylinder for both the constant (Theorem 7.1) and affine (Theorem 7.2 as stated below) cases.

Theorem 7.2 (Affine Dynamics Stability) *Let $\mathbf{F} \in \mathcal{A}_3$ be given by (37) with $\gamma_i \neq 0$. Given $\Sigma_{\theta_0} \in \tilde{\mathcal{I}}_C$, let $\mathbf{X} = (\mathbf{X}_-, \mathbf{X}_+)$ be the Filippov system induced around Σ_{θ_0} and inside a convex compact set $K \subset C_+ \cup C_-$, where C_+ and C_- are two consecutive stripes meeting at Σ_{θ_0} . Then, \mathbf{F} is (Σ_{θ_0}, K) -semi-local structurally stable in \mathcal{A}_3 if, and only if, \mathbf{X}_+ and \mathbf{X}_- satisfies*

1. $a_{i1} \neq 0$ and $\mathbf{P} \notin \Sigma_{\theta_0}$, where \mathbf{P} is the only singularity of \mathbf{X}_{\pm} ;
2. conditions (C.6) — (C.9) of Proposition 7.2.

For clarification on the technicalities involved, especially in the statement above, we encourage the interested reader to please consult the respective section in the text, which is structured as follows: preliminaries are presented in Section 2, followed by a formal statement of the problem in Section 3 and then the methodology in Section 4 – general results for the non-linear case are also contained here as consequences of the fundamental dynamics obtained. Next,

when generated by constant and affine vector fields, a complete qualitative description of the fundamental dynamics are obtained in Sections 5 and 6, respectively. Finally, in Section 7, this fine-grained control of the fundamental dynamics is leveraged to derive Peixoto-like theorems characterizing semi-local structural stability. Conclusion, in Section 8, contains some final thoughts and further directions of investigation.

A preliminar version of this paper can be found archived in [39].

2 Preliminaries

In this section, we introduce the concept of regularization developed by Jorge Sotomayor and Marco Antonio Teixeira in [40]. First, given a piecewise vector field, we construct its regularization, which consists of a 1-parameter family of smooth vector fields which converges to the given piecewise field. Next, we introduce part of the Geometrical Singular Perturbation Theory developed by Neil Fenichel in [19] and its connection with Filippov dynamics through regularization.

2.1 Sotomayor-Teixeira regularization

Let $\mathbf{F} = (\mathbf{F}_+, \mathbf{F}_-) \in \mathcal{R}^k(U)$ be a piecewise smooth vector field as defined above with a switching manifold $\Sigma = h^{-1}(0)$. A Sotomayor-Teixeira regularization of \mathbf{F} , as described at [40], is a 1-parameter family of smooth vector fields \mathbf{F}^ε that converges pointwisely to \mathbf{F} as $\varepsilon \rightarrow 0$. More precisely, for $\mathbf{x} \in U \setminus \Sigma$, observe that the field \mathbf{F} can be written in the form

$$\mathbf{F}(\mathbf{x}) = \left[\frac{1 + \operatorname{sgn}(h(\mathbf{x}))}{2} \right] \mathbf{F}_+(\mathbf{x}) + \left[\frac{1 - \operatorname{sgn}(h(\mathbf{x}))}{2} \right] \mathbf{F}_-(\mathbf{x}), \quad (7)$$

where $\operatorname{sgn} : \mathbb{R} \rightarrow \mathbb{R}$ is the **signal function** given by

$$\operatorname{sgn}(x) = \begin{cases} -1, & \text{if } x < 0, \\ 0, & \text{if } x = 0, \\ 1, & \text{if } x > 0, \end{cases}$$

which is a discontinuous function whose graph is represented at Figure 4a.

In order to approximate the piecewise smooth vector \mathbf{F} with a 1-parameter family of smooth vector fields, we approximate the signal function at (7) with a certain type of smooth function. More precisely:

Definition 2.1 We say that a smooth function $\varphi : \mathbb{R} \rightarrow \mathbb{R}$ is a **monotonous² transition function** if

$$\varphi(x) = \begin{cases} -1, & \text{if } x \leq -1, \\ 1, & \text{if } x \geq 1, \end{cases}$$

and $\varphi'(x) > 0$ for $-1 < x < 1$.

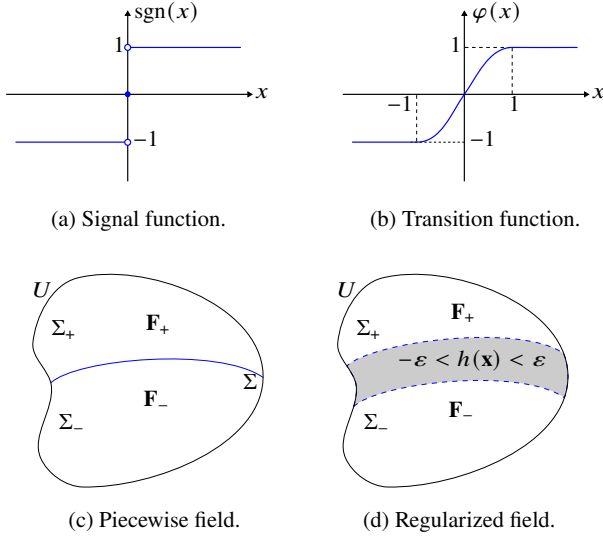


Fig. 4: Grid representation of the Sotomayor-Teixeira's regularization with the signal function (a) associated to the piecewise smooth vector field (c) and the transition function (b) associated to the regularized vector field (d).

The graph of a typical transition function is represented at Figure 4b. Observe that, if we define $\varphi^\varepsilon(x) = \varphi\left(\frac{x}{\varepsilon}\right)$, where $\varepsilon > 0$, then clearly $\varphi^\varepsilon \rightarrow \text{sgn}$ pointwisely when $\varepsilon \rightarrow 0$, as long as their domains are restricted to the set $\mathbb{R} \setminus \{0\}$. In particular, if we define

$$\mathbf{F}^\varepsilon(\mathbf{x}) = \left[\frac{1 + \varphi^\varepsilon(h(\mathbf{x}))}{2} \right] \mathbf{F}_+(\mathbf{x}) + \left[\frac{1 - \varphi^\varepsilon(h(\mathbf{x}))}{2} \right] \mathbf{F}_-(\mathbf{x}), \quad (8)$$

then we get a 1-parameter family of vector fields $\mathbf{F}^\varepsilon \in C^k(U)$ such that $\mathbf{F}^\varepsilon \rightarrow \mathbf{F}$ pointwisely when $\varepsilon \rightarrow 0$, as long as their domains are restricted to the set $\mathbb{R} \setminus \{0\}$.

Definition 2.2 Let $\varphi : \mathbb{R} \rightarrow \mathbb{R}$ be a monotonous transition function. We say that (8) is a φ^ε -**regularization** of (7).

² A study on the regularization process with non-monotonous transition functions can be found at the chapter 6 of [34].

Observe that the regularization \mathbf{F}^ε coincides with \mathbf{F} outside the rectangle given by $-\varepsilon < h(\mathbf{x}) < \varepsilon$. In fact,

$$\mathbf{F}^\varepsilon(\mathbf{x}) = \begin{cases} \mathbf{F}_+(\mathbf{x}), & \text{if } h(\mathbf{x}) \geq \varepsilon, \\ \mathbf{F}_-(\mathbf{x}), & \text{if } h(\mathbf{x}) \leq -\varepsilon, \end{cases}$$

as represented at Figure 4d. In particular, it is clear that \mathbf{F}^ε recovers the smooth component of the Filippov dynamics given by \mathbf{F} , i.e., that associated to the region $U \setminus \Sigma$, as long as we take $\varepsilon > 0$ small enough. As described in the next section, \mathbf{F}^ε also recovers the non-smooth component of the Filippov dynamics, i.e., that associated to the region Σ .

2.2 Geometrical Singular Perturbation Theory

Let $W \subset \mathbb{R}^{m+n}$ be an open set whose elements are represented by (\mathbf{x}, \mathbf{y}) . Let also $\mathbf{f} : W \times [0, 1] \rightarrow \mathbb{R}^m$ and $\mathbf{g} : W \times [0, 1] \rightarrow \mathbb{R}^n$ be vector fields of class C^k with $k \geq 1$. Given $0 < \xi < 1$, consider the system of differential equations

$$\begin{cases} \dot{\mathbf{x}}' = \mathbf{f}(\mathbf{x}, \mathbf{y}, \xi) \\ \dot{\mathbf{y}}' = \xi \mathbf{g}(\mathbf{x}, \mathbf{y}, \xi) \end{cases}, \quad (9)$$

where $\dot{\square}' = d\square/dt$, $\mathbf{x} = \mathbf{x}(\tau)$ and $\mathbf{y} = \mathbf{y}(\tau)$. Applying at the previous system the time rescaling given by $t = \xi\tau$, we obtain the new system

$$\begin{cases} \xi \dot{\mathbf{x}} = \mathbf{f}(\mathbf{x}, \mathbf{y}, \xi) \\ \dot{\mathbf{y}} = \mathbf{g}(\mathbf{x}, \mathbf{y}, \xi) \end{cases}, \quad (10)$$

where $\dot{\square} = d\square/dt$, $\mathbf{x} = \mathbf{x}(t)$ and $\mathbf{y} = \mathbf{y}(t)$.

As $0 < \xi < 1$, then (9) and (10) have exactly the same phase portrait, except for the trajectories speed, which is greater for first system and smaller for the second. Therefore, the following definition makes sense:

Definition 2.3 We say that (9) and (10) form a (m, n) -**slow-fast system** with **fast system** given by (9) and **slow system** given by (10).

Taking $\xi \rightarrow 0$ in (9), we get the so-called **layer system**

$$\begin{cases} \dot{\mathbf{x}}' = \mathbf{f}(\mathbf{x}, \mathbf{y}, 0) \\ \dot{\mathbf{y}}' = \mathbf{0} \end{cases}, \quad (11)$$

which has dimension m . Taking $\xi \rightarrow 0$ in (10), we get the so-called **reduced system**

$$\begin{cases} \dot{\mathbf{0}} = \mathbf{f}(\mathbf{x}, \mathbf{y}, 0) \\ \dot{\mathbf{y}} = \mathbf{g}(\mathbf{x}, \mathbf{y}, 0) \end{cases}, \quad (12)$$

which has dimension n . Beyond that, we say that the set

$$\mathcal{M} = \{(\mathbf{x}, \mathbf{y}) \in W; \mathbf{f}(\mathbf{x}, \mathbf{y}, 0) = \mathbf{0}\}$$

is the **slow manifold**. Observe that, on one hand, \mathcal{M} represents the set of singularities of the layer system; on the other hand, \mathcal{M} represents the manifold over which the dynamics of the reduced system takes place.

The main idea of Geometrical Singular Perturbation Theory, or GSP-Theory for short, established by Fenichel in [19], consists of combining the dynamics of the limit systems (layer and reduced) to recover the dynamics of the initial system (slow-fast) with $\xi > 0$ small. In fact, considering ξ as an additional variable of the slow system (10) we get the new one

$$\begin{cases} \mathbf{x}' = \mathbf{f}(\mathbf{x}, \mathbf{y}, \xi) \\ \mathbf{y}' = \xi \mathbf{g}(\mathbf{x}, \mathbf{y}, \xi) \\ \xi' = 0 \end{cases} \quad (13)$$

whose Jacobian matrix at $(\mathbf{x}_0, \mathbf{y}_0, 0) \in \mathcal{M} \times \{0\}$ is

$$\mathbf{J}_{\text{fast}} = \begin{bmatrix} \mathbf{f}_x & \mathbf{f}_y & 0 \\ \mathbf{0} & \mathbf{0} & 0 \\ \mathbf{0} & \mathbf{0} & 0 \end{bmatrix}, \quad (14)$$

where \mathbf{f}_x and \mathbf{f}_y represent the partial derivatives calculated at the point $(\mathbf{x}_0, \mathbf{y}_0, 0)$. The matrix above has the trivial eigenvalue $\lambda = 0$ with algebraic multiplicity $n + 1$. The remaining eigenvalues, called **non-trivial**, are divided in three categories: negative, zero or positive real parts; we denote the number of such eigenvalues by k^s , k^c and k^u , respectively.

Definition 2.4 We say that $(\mathbf{x}_0, \mathbf{y}_0, 0) \in \mathcal{M} \times \{0\}$ is **normally hyperbolic** if every non-trivial eigenvalue of (14) have non-zero real part, i.e., $k^c = 0$.

Fenichel, in [19], proved that normal hyperbolicity allows the persistence of invariant compact parts of the slow manifold under singular perturbation, i.e., the dynamical structure of such parts with $\xi = 0$ persists for $\xi > 0$ small. Even more, with predictable stability. More precisely:

Theorem 2.1 (Retrieved from [43], page 1953) *Let \mathcal{N} be a normally hyperbolic compact invariant j -dimensional submanifold of \mathcal{M} . Suppose that the stable and unstable manifolds of \mathcal{N} , with respect to the reduced system, have dimensions $j + j^s$ and $j + j^u$, respectively. Then, there exists a 1-parameter family of invariant submanifolds $\{\mathcal{N}_\xi; \xi \sim 0\}$ such that $\mathcal{N}_0 = \mathcal{N}$ and \mathcal{N}_ξ has stable and unstable manifolds with dimensions $j + j^s + k^s$ and $j + j^u + k^u$, respectively.*

The reverse idea of GSP-Theory can also be used to recover the non-smooth component of the Filippov dynamics,

given by the piecewise vector field ($\varepsilon = 0$), from its regularization ($\varepsilon > 0$). In fact, let $\mathbf{F} = (\mathbf{F}_+, \mathbf{F}_-) \in \mathcal{R}^k(U, h)$ be a piecewise smooth vector field with switching manifold $\Sigma = h^{-1}(\{0\})$. Let also $\varphi : \mathbb{R} \rightarrow \mathbb{R}$ be a monotonous transition function and \mathbf{F}^ε the φ^ε -regularization of \mathbf{F} .

We need to transform \mathbf{F}^ε in a slow-fast system. In order to do so, observe that, as 0 is a regular value of h , then from the Local Normal Form for Submersions follows that, without loss of generality, we can admit that $h(x_1, \dots, x_n) = x_1$ in a neighborhood of a given point $\mathbf{x} \in \Sigma$. Therefore, if we write $\mathbf{F}_+ = (f_1^+, \dots, f_n^+)$ and $\mathbf{F}_- = (f_1^-, \dots, f_n^-)$, then follows that \mathbf{F}^ε can be written as

$$\dot{x}_i = \left[\frac{1 + \varphi^\varepsilon(x_1)}{2} \right] f_i^+(x_1, \dots, x_n) + \left[\frac{1 - \varphi^\varepsilon(x_1)}{2} \right] f_i^-(x_1, \dots, x_n),$$

where $i \in \{1, \dots, n\}$. Now, applying to the system above the polar blow-up given by $x_1 = \xi \cos \theta$ and $\varepsilon = \xi \sin \theta$, where $\xi \geq 0$ and $\theta \in [0, \pi]$, we obtain a $(1, n - 1)$ -slow-fast system given by

$$\begin{cases} \xi \dot{\theta} = \alpha_1(\theta, x_2, \dots, x_n, \xi) \\ \dot{x}_i = \alpha_i(\theta, x_2, \dots, x_n, \xi) \end{cases}, \quad (15)$$

where $i \in \{2, \dots, n\}$.

Observe that, for $\xi = 0$, we have $x_1 = 0$ and $\varepsilon = 0$, i.e., we are at the non-regularized system \mathbf{F} over the manifold Σ . In the other hand, for $\xi > 0$ and $\theta \in (0, \pi)$, we have $-\xi < x_1 < \xi$ and $0 < \varepsilon < \xi$, i.e., we are at the regularized system \mathbf{F}^ε over the rectangle where it does not coincide to \mathbf{F} , see Figure 4d. The authors of [43] then proved the result below:

Theorem 2.2 (Retrieved from [43], page 1950) *Consider the piecewise smooth vector field \mathbf{F} and the slow-fast system (15). The sliding region Σ^s is homeomorphic to the slow manifold given by*

$$\alpha_1(\theta, x_2, \dots, x_n, 0) = 0$$

and the dynamics of the sliding vector field \mathbf{F}^s over Σ^s is topologically equivalent to that of the reduced system given by

$$\begin{cases} 0 = \alpha_1(\theta, x_2, \dots, x_n, 0) \\ \dot{x}_i = \alpha_i(\theta, x_2, \dots, x_n, 0) \end{cases},$$

where $i \in \{2, \dots, n\}$.

Concisely, the Filippov dynamics of \mathbf{F} is completely recovered by its regularization \mathbf{F}^ε . In order to do so, the following steps, described in details above, are necessary:

1. Normalization of the switching manifold.
2. Regularization of the piecewise smooth vector field.
3. Polar blow-up of the regularization.
4. Analysis of the resulting limit systems (layer and reduced).

3 Statement of the Problem

One of the fundamental hypotheses in the theory described in Section 1 is the fact that $0 \in \mathbb{R}$ is a **regular value** of the function $h : \mathbb{R} \rightarrow \mathbb{R}$ and, therefore, the switching manifold $\Sigma = h^{-1}(\{0\})$ is a regular surface. In that case, as we have seen, there exists at least one well-defined and established dynamics associated: the Filippov dynamics. A natural question to ask then is: can a Filippov-like dynamics be defined for the case when $0 \in \mathbb{R}$ is a **singular value** of the function $h : \mathbb{R} \rightarrow \mathbb{R}$, i.e., when the switching manifold is not a regular surface?

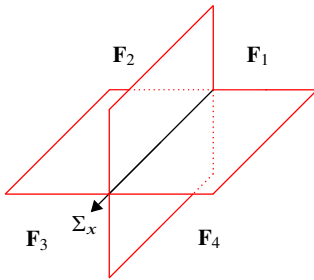


Fig. 5: Double discontinuity.

In the next sections, we would like to study the particular case known as the **double discontinuity**. This particular configuration of the switching manifold is the simplest one between the four singular configurations (known as Gutierrez-Sotomayor or simple manifolds) that, according to [24], breaks the regularity condition in a dynamically stable manner. The double discontinuity is described in detail below.

Let $\mathbf{F}_i : \mathbb{R}^3 \rightarrow \mathbb{R}^3$ be vector fields of class $C^k(\mathbb{R}^3)$ with $i \in \{1, 2, 3, 4\}$. The piecewise smooth vector field $\mathbf{F} : \mathbb{R}^3 \rightarrow \mathbb{R}^3$ given by

$$\mathbf{F}(x, y, z) = \begin{cases} \mathbf{F}_1(x, y, z), & \text{if } y \geq 0 \text{ and } z \geq 0, \\ \mathbf{F}_2(x, y, z), & \text{if } y \leq 0 \text{ and } z \geq 0, \\ \mathbf{F}_3(x, y, z), & \text{if } y \leq 0 \text{ and } z \leq 0, \\ \mathbf{F}_4(x, y, z), & \text{if } y \geq 0 \text{ and } z \leq 0, \end{cases} \quad (16)$$

and denoted by $\mathbf{F} = (\mathbf{F}_1, \mathbf{F}_2, \mathbf{F}_3, \mathbf{F}_4)$ is said to have a **double discontinuity** as switching manifold, see Figure 5. The set of all vector fields \mathbf{F} defined as above will be denoted by

$$\mathcal{D}_3^k \equiv C^k(\mathbb{R}^3) \times C^k(\mathbb{R}^3) \times C^k(\mathbb{R}^3) \times C^k(\mathbb{R}^3)$$

and equipped with the Whitney product topology.

The double discontinuity, as defined above, consists of the planes xy and xz perpendicularly intersecting at the x -axis, $\Sigma_x = \{(x, 0, 0); x \in \mathbb{R}\}$. For points in $\Sigma \setminus \Sigma_x$, the ordinary Filippov dynamics described in Section 1 can be locally applied. However, for points $(x, 0, 0) \in \Sigma_x$ that theory cannot be directly applied. In fact, $\Sigma = h^{-1}(\{0\})$, where $h : \mathbb{R}^3 \rightarrow \mathbb{R}$ given by $h(x, y, z) = yz$ has $0 \in \mathbb{R}$ as a singular value, since $Dh(x, 0, 0)$ is not a surjective map for $(x, 0, 0) \in \Sigma_x$.

Therefore, we state the problem: given $\mathbf{F} \in \mathcal{D}_3^k$, can we define a Filippov-like dynamics over Σ_x ? How does it generally behave there? In the next section, we present a methodology based on [8, 33, 36, 43] to approach this problem.

4 Methodology

The first step consists of the application of a polar blow-up at the origin of the slice represented at Figure 6a or, in other words, a **cylindrical blow-up** at Σ_x . More specifically, assuming that the components of $\mathbf{F} \in \mathcal{D}_3^k$ can be written as

$$\mathbf{F}_i = (w_i, p_i, q_i),$$

we apply the blow-up $\phi_1 : \mathbb{R} \times S^1 \times \mathbb{R}^+ \rightarrow \mathbb{R}^3$ given by

$$\phi_1(x, \theta, r) = (x, r \cos \theta, r \sin \theta),$$

which induces $\tilde{\mathbf{F}} = [(\phi_1)_*^{-1} \mathbf{F}] \circ \phi_1$ whose components are given by

$$\tilde{\mathbf{F}}_i = \left(w_i, \frac{q_i \cos \theta - p_i \sin \theta}{r}, p_i \cos \theta + q_i \sin \theta \right),$$

where w_i, p_i and q_i must be evaluated at the point $\phi_1(x, \theta, r)$. We then define the set

$$\tilde{\mathcal{D}}_3^k = \{\tilde{\mathbf{F}} = [(\phi_1)_*^{-1} \mathbf{F}] \circ \phi_1; \mathbf{F} \in \mathcal{D}_3^k\}$$

of all blow-up induced vector fields.

An extremely important observation at this point consists in the theorem stated below with minor adaptations to our notation relative to the original one found in [33]³

³ Up to our knowledge, this theorem where actually first stated in [8, p. 449]. However, [33] also provides analogous results for the triple, cone, and Whitney discontinuities. See Figure 1. Regarding the double discontinuity, similar versions of the theorem can also be found

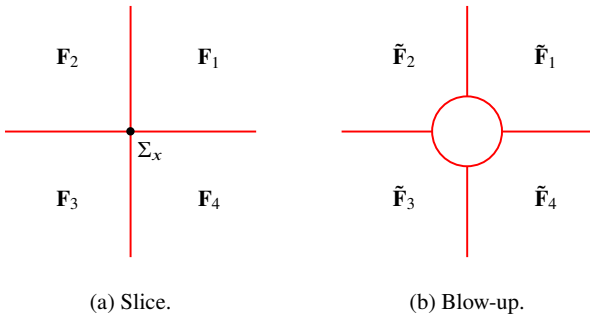


Fig. 6: Framework process at slice-level.

Theorem 4.1 (Retrieved from [33], page 498) *The map $\phi_1 : \mathbb{R} \times S^1 \times \mathbb{R}^+ \rightarrow \mathbb{R}^3$ given by*

$$\phi_1(x, \theta, r) = (x, r \cos \theta, r \sin \theta)$$

induces a vector field $\tilde{\mathbf{F}}$ satisfying that any discontinuity $q \in \tilde{\Sigma} = \phi_1^{-1}(\Sigma)$ is regular.

Hence, since the induced vector field $\tilde{\mathbf{F}}$ has only **regular discontinuities**, then classical Filippov theory, as presented at Section 1, is enough for its analysis. More precisely, we have now a piecewise smooth vector field $\tilde{\mathbf{F}}$ given by the four smooth vector fields $\tilde{\mathbf{F}}_i$, which induces the four **slow-fast systems**

$$\begin{cases} \dot{x} = w_i \\ r\dot{\theta} = q_i \cos \theta - p_i \sin \theta, \\ \dot{r} = p_i \cos \theta + q_i \sin \theta \end{cases} \quad (17)$$

where $\dot{\square} = d\square/dt$; w_i , p_i and q_i must be calculated at the point $\phi_1(x, \theta, r)$; and r is the time rescaling factor.

The study of the dynamics of (16) has therefore been reduced to the study of the slow-fast systems (17). In particular, the dynamics over Σ_x , previously undefined, can now be associated with (17) at $r = 0$, which is given by the combination of the dynamics of the **reduced system**

$$\begin{cases} \dot{x} = w_i \\ 0 = q_i \cos \theta - p_i \sin \theta \\ \dot{r} = p_i \cos \theta + q_i \sin \theta \end{cases} \quad (18)$$

and the dynamics of the **layer system**

$$\begin{cases} x' = 0 \\ \theta' = q_i \cos \theta - p_i \sin \theta, \\ r' = 0 \end{cases} \quad (19)$$

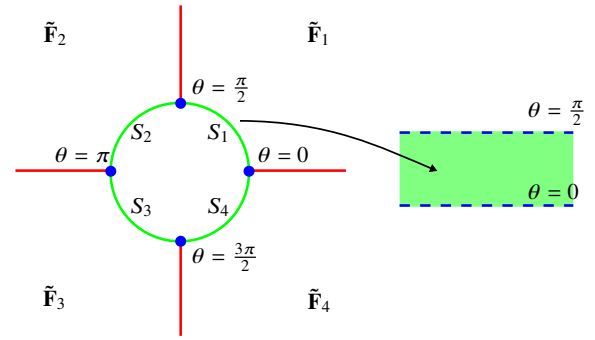
in [36], within the context of foliations, and in [43], which is actually a survey. Besides that, as raised in Section 1, this theorem (with some sparse examples) represents the state of the art. **In other words, results following the statement are novelties on a sparsely explored territory.**

where $\square' = d\square/d\tau$ with $t = r\tau$; and the components w_i , p_i and q_i must be calculated at the point $\phi_1(x, \theta, 0) = (x, 0, 0)$.

Geometrically, the dynamics over Σ_x in (16) can now be associated to the dynamics over the cylinder $C = \mathbb{R} \times S^1$ divided in the four infinite stripes

$$\begin{aligned} S_2 &= \mathbb{R} \times [\pi/2, \pi], & S_1 &= \mathbb{R} \times [0, \pi/2], \\ S_3 &= \mathbb{R} \times [\pi, 3\pi/2], & S_4 &= \mathbb{R} \times [3\pi/2, 2\pi], \end{aligned}$$

as represented at Figure 7, where the slow-fast systems given by (18) and (19) acts, respectively. As we previously stated at Theorem 4.1, the four lines where these stripes intersect admits at most regular discontinuities. Finally, the analysis of the dynamics on each stripe S_i can then be carried out using GSP-Theory.

Fig. 7: Green cylinder C divided in the four stripes S_i . A scheme of the stripe S_1 is also put in evidence.

In particular, the first two equations of the system (18) are independent of r and, therefore, it can be decoupled as

$$\begin{cases} \dot{x} = w_i \\ 0 = q_i \cos \theta - p_i \sin \theta \end{cases} \quad (20)$$

which gives the **reduced dynamics** over S_i ; and

$$\dot{r} = p_i \cos \theta + q_i \sin \theta, \quad (21)$$

which gives the respective **slow radial dynamics** or, in other words, it indicates how the external dynamics communicates with the dynamics (20) over the cylinder: entering ($\dot{r} > 0$), leaving ($\dot{r} < 0$) or staying ($\dot{r} = 0$) at S_i .

Analogously, the first two equations of the system (19) are independent of r and, therefore, it can also be decoupled as

$$\begin{cases} x' = 0 \\ \theta' = q_i \cos \theta - p_i \sin \theta \end{cases} \quad (22)$$

which gives the **layer dynamics** over S_i ; and

$$r' = 0, \quad (23)$$

which gives the respective **fast radial dynamics** over the cylinder.

Summarizing, we conclude that the dynamics over Σ_x behaves as described in the **fundamental lemma** below, whose proof consists in the analysis done above.

Lemma 4.1 (Fundamental Dynamics) *Given $\mathbf{F} \in \mathcal{D}_3^k$ with components $\mathbf{F}_i = (w_i, p_i, q_i)$, let $\tilde{\mathbf{F}} \in \tilde{\mathcal{D}}_3^k$ be the vector field induced by the blow-up*

$$\phi_1(x, \theta, r) = (x, r \cos \theta, r \sin \theta).$$

Then, this blow-up associates the dynamics over Σ_x with the following dynamics over the cylinder $C = \mathbb{R} \times S^1 = S_1 \cup \dots \cup S_4$: over each stripe S_i acts a slow-fast dynamics whose reduced dynamics is given by

$$\begin{cases} \dot{x} = w_i \\ 0 = q_i \cos \theta - p_i \sin \theta \end{cases} \quad (24)$$

with slow radial dynamics $\dot{r} = p_i \cos \theta + q_i \sin \theta$; and layer dynamics given by

$$\begin{cases} x' = 0 \\ \theta' = q_i \cos \theta - p_i \sin \theta \end{cases} \quad (25)$$

with fast radial dynamics $r' = 0$. Finally, at every equation above the functions w_i , p_i and q_i must be calculated at the point $\phi_1(x, \theta, 0) = (x, 0, 0)$.

In order to perform a deeper analysis of the dynamics given by Lemma 4.1 with GSP-Theory as described at Section 2.2, let S_i be one of the cylinder's stripe and let

$$\mathcal{M}_i = \{(x, \theta) \in S_i \subset \mathbb{R} \times S^1; f_i(x, \theta, 0) = 0\}$$

be its slow manifold, where $f_i(x, \theta, 0) = q_i \cos \theta - p_i \sin \theta$.

Given $(x_0, \theta_0, 0) \in \mathcal{M}_i \times \{0\}$, the Jacobian matrix of the complete layer system (19) over this point is

$$\mathbf{J}_{\text{fast}} = \begin{bmatrix} 0 & 0 & 0 \\ (f_i)_x & (f_i)_\theta & 0 \\ 0 & 0 & 0 \end{bmatrix},$$

where $(f_i)_x$ and $(f_i)_\theta$ represents the partial derivatives calculated at $(x_0, \theta_0, 0)$. The eigenvalues of this matrix are the elements of the set $\{0, 0, (f_i)_\theta\}$ and, therefore, (x_0, θ_0) is normally hyperbolic if, and only if, $(f_i)_\theta \neq 0$. However,

we observe that, since we are over the slow manifold, then $(f_i)_\theta = 0$ leads to the homogeneous linear system

$$\begin{cases} f_i = 0 \\ (f_i)_\theta = 0 \end{cases} \sim \begin{cases} q_i \cos \theta - p_i \sin \theta = 0 \\ q_i \sin \theta + p_i \cos \theta = 0 \end{cases} \sim \begin{cases} \cos \theta - \sin \theta \\ \sin \theta \cos \theta \end{cases} \begin{bmatrix} q_i \\ p_i \end{bmatrix} = \begin{bmatrix} 0 \\ 0 \end{bmatrix}$$

whose unique solution is the trivial, $p_i = q_i = 0$, since the trigonometrical matrix above is invertible ($\det \equiv 1$) for every $\theta \in S^1$ and, therefore, we conclude that $(f_i)_\theta \neq 0$ whenever

$$p_i \neq 0 \quad \text{or} \quad q_i \neq 0, \quad (\text{WFH})$$

henceforth, called **weak fundamental hypothesis**, or WFH for short. We also observe that

$$(f_i)_x = (q_i)_x \cos \theta - (p_i)_x \sin \theta$$

which, as above, supposing $(f_i)_x = 0$ leads to the homogeneous linear system

$$\begin{cases} q_i \cos \theta - p_i \sin \theta = 0 \\ (q_i)_x \cos \theta - (p_i)_x \sin \theta = 0 \end{cases} \sim \begin{cases} q_i & p_i \\ (q_i)_x & (p_i)_x \end{cases} \begin{bmatrix} \cos \theta \\ \sin \theta \end{bmatrix} = \begin{bmatrix} 0 \\ 0 \end{bmatrix}$$

which only admits the absurd solution $\cos \theta = \sin \theta = 0$ if the matrix above is invertible. Hence, we can ensure $(f_i)_x \neq 0$ by imposing this absurd, i.e.,

$$0 \neq \det \begin{bmatrix} q_i & p_i \\ (q_i)_x & (p_i)_x \end{bmatrix} = q_i(p_i)_x - p_i(q_i)_x \quad (\text{SFH})$$

which always implies the weak fundamental hypothesis and, therefore, will be called **strong fundamental hypothesis**, or SFH for short.

Theorem 4.2 *The radial dynamics can only be transversal ($\dot{r} \neq 0$) to the cylinder C over the slow manifold \mathcal{M}_i . More over, under (WFH), it is in fact transversal.*

Proof The first part of the statement is assured by Lemma 4.1. For the second part, just observe that $\dot{r} = -(f_i)_\theta \neq 0$ under (WFH).

Theorem 4.3 *The slow manifold \mathcal{M}_i is locally a graph $(x, \theta(x))$ under (WFH). However, if $\|(f_i)_\theta\|$ admits a global positive minimum, then \mathcal{M}_i is globally a graph $(x, \theta(x))$. Either way, $\theta(x)$ is of class C^k .*

Proof The first part is assured by the usual Implicit Function Theorem applied to $f_i(x_0, \theta_0, 0) = 0$ over \mathcal{M}_i , since under (WFH) we have $\|(f_i)_\theta\| > 0$. Analogously, the second part is assured by the Global Implicit Function Theorem found in [51, p. 253], which requires a stronger hypothesis.

Theorem 4.4 *The slow manifold \mathcal{M}_i is normally hyperbolic at every point that satisfies (WFH).*

Proof Just observe that $(f_i)_\theta$, the only non-trivial eigenvalue, is non-zero under (WFH).

Theorem 4.5 *The hyperbolic singularities of the reduced system (24) acts as hyperbolic saddle or node singularities of S_i under (WFH).*

Proof Let $\mathbf{P} = (x_0, \theta_0) \in \mathcal{M}_i$ be a hyperbolic singularity of the reduced system, i.e., $w_i(x_0, 0, 0) = 0$ with eigenvalue $\lambda_1 = (w_i)_x(x_0, 0, 0) \neq 0$. We have two possibilities:

- $\lambda_1 > 0 \Rightarrow (j^s, j^u) = (0, 1)$; or
- $\lambda_1 < 0 \Rightarrow (j^s, j^u) = (1, 0)$,

where j^s and j^u are the dimensions of the stable and unstable manifolds of \mathbf{P} with respect to the reduced system, respectively.

On the other hand, under (WFH) we also have the non-trivial eigenvalue $\lambda_2 = (f_i)_\theta(x_0, \theta_0, 0) \neq 0$ for the layer system and, therefore, the two possibilities:

- $\lambda_2 > 0 \Rightarrow (k^s, k^u) = (0, 1)$; or
- $\lambda_2 < 0 \Rightarrow (k^s, k^u) = (1, 0)$,

where k^s and k^u are the dimensions of the stable and unstable manifolds of \mathbf{P} with respect to the layer system, respectively.

Hence, observing that $j = \dim \mathbf{P} = 0$ and remembering Theorem 2.1, any combination of the signs of λ_1 and λ_2 leads to the total sum of dimensions

$$(j^s + k^s) + (j^u + k^u) = 2 = \dim S_i,$$

and, therefore, \mathbf{P} acts as a hyperbolic singularity of S_i . Finally, the saddle-node duality comes from the fact that both non-trivial eigenvalues above have no imaginary parts.

In other words, under (WFH), the slow manifold \mathcal{M}_i is, at the very least, locally a graph. More than that, it is the entry-point for the external dynamics to the cylinder. Besides that, it is normally hyperbolic at its full extension, assuring then not only persistence and well-behaved stability for its invariant compact parts, but also that \mathcal{M}_i is always attracting or repelling the surrounding (layer) dynamics. All these nice properties come at the low cost of (WFH). Therefore, it is not a surprise that, for every system studied below, we require at least (WFH), but also always test for (SFH), whose importance will become clear when studying affine systems.

5 Constant Dynamics

Let $\mathcal{C}_3 \subset \mathcal{D}_3^k$ be the set of all piecewise smooth vector fields \mathbf{F} with a double discontinuity given by constant vector fields

$$\mathbf{F}_i(x, y, z) = (d_{i1}, d_{i2}, d_{i3}), \quad (26)$$

where $d_{ij} \in \mathbb{R}$ for all i and j . According to the Fundamental Lemma 4.1, the dynamics over Σ_x of such a field is blow-up associated to the following fundamental dynamics over the cylinder $C = \mathbb{R} \times S^1 = S_1 \cup \dots \cup S_4$: over each stripe S_i acts a slow-fast dynamics whose reduced dynamics is given by

$$\begin{cases} \dot{x} = d_{i1} \\ 0 = d_{i3} \cos \theta - d_{i2} \sin \theta \end{cases} \quad (27)$$

with radial slow dynamics $\dot{r} = d_{i2} \cos \theta + d_{i3} \sin \theta$; and layer dynamics given by

$$\begin{cases} x' = 0 \\ \theta' = d_{i3} \cos \theta - d_{i2} \sin \theta \end{cases} \quad (28)$$

with radial fast dynamics $r' = 0$.

Besides that, for (26), we have $p_i = d_{i2}$ and $q_i = d_{i3}$ so that (WFH) is satisfied as long as

$$d_{i2} \neq 0 \quad \text{or} \quad d_{i3} \neq 0, \quad (29)$$

whereas (SFH) is **never** satisfied, since $(p_i)_x = (q_i)_x = 0$.

Therefore, our goal at this section is to fully describe the fundamental dynamics of (26) over the cylinder C under the hypothesis (29). In order to do so, we are going to systematically analyze the slow-fast systems (27)–(28) for the cases suggested by (29). This analysis takes place in Sections 5.1 and 5.2, resulting in Theorem 5.1 stated and exemplified at Section 5.3.

5.1 Case $d_{i2} \neq 0$

In order to explicitly define the slow manifold \mathcal{M}_i , observe that whenever $\cos \theta \neq 0$ the second equation of (27) gives us

$$0 = d_{i3} \cos \theta - d_{i2} \sin \theta \Leftrightarrow \tan \theta = \frac{d_{i3}}{d_{i2}} \Leftrightarrow$$

$$\Leftrightarrow \theta = \arctan\left(\frac{d_{i3}}{d_{i2}}\right) + n\pi = \theta_i + n\pi,$$

where $n \in \mathbb{Z}$. Therefore, without loss of generality, the slow manifold can be written as $\mathcal{M}_i = L_i \cup L_i^\pi$, where

$$\begin{aligned} L_i &= \{(x, \theta) \in \mathbb{R} \times [0, 2\pi]; \theta = \theta_i\} \text{ and} \\ L_i^\pi &= \{(x, \theta) \in \mathbb{R} \times [0, 2\pi]; \theta = \theta_i + \pi\}, \end{aligned}$$

which consists of two straight lines inside the cylinder $C = \mathbb{R} \times [0, 2\pi]$, as the red part of Figure 8. In fact, *a priori*, \mathcal{M}_i is a subset of the particular stripe S_i . However, since the subjacent vector fields, (26), are defined for every point of \mathbb{R}^3 , then, without any mathematical restriction or weakness, we can consider \mathcal{M}_i as a subset of the whole cylinder C , not restricted to the particular stripe S_i , in order to study its properties. Once this global analysis is done, we can then focus on the particular stripe of interest.

In particular, since $\theta_i \in (-\frac{\pi}{2}, \frac{\pi}{2})$ and $\theta_i + \pi \in (\frac{\pi}{2}, \frac{3\pi}{2})$, then either $L_i \subset S_1$ and $L_i^\pi \subset S_3$ or $L_i \subset S_4$ and $L_i^\pi \subset S_2$. In other words, these straight lines are always at intercalated stripes. Therefore, a given stripe S_i might or might not contain one of these straight lines, depending exclusively on the value of θ_i .⁴ This completes the qualitative analysis of the shape of the slow manifold.

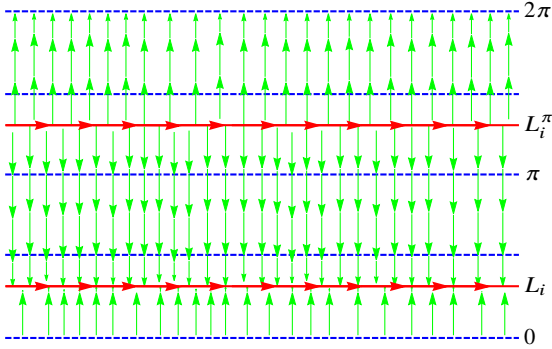


Fig. 8: Constant double discontinuity dynamics for $d_{i1} = 1 > 0$, $d_{i2} = 0.7 > 0$ and $d_{i3} = 1 > 0$. At this example we have $\theta_i = \arctan \frac{1}{0.7} \approx 0.96$. Therefore, for example, S_1 has $\theta = \theta_i$ as an attracting visible part of the slow manifold; whereas S_2 has none.

Over both the straight lines $\mathcal{M}_i = L_i \cup L_i^\pi$, we have the one-dimensional dynamics given by the first equation of (27), i.e., $\dot{x} = d_{i1}$. Analyzing this equation we observe that, considering the usual growth direction of the x -axis, the dynamics over \mathcal{M}_i is increasing if $d_{i1} > 0$ and decreasing if $d_{i1} < 0$. This completes the qualitative analysis of the reduced dynamics.

Regarding the layer dynamics, we have the layer system (28) which says that for each fixed value of $x \in \mathbb{R}$, we have a one-dimensional dynamics given by the second equation of (28). In particular, assuming that $\cos \theta > 0$ and $d_{i2} > 0$, then

$$\theta' > 0 \Leftrightarrow d_{i3} \cos \theta - d_{i2} \sin \theta > 0 \Leftrightarrow \tan \theta < \frac{d_{i3}}{d_{i2}} \Leftrightarrow$$

$$\Leftrightarrow \theta < \arctan \left(\frac{d_{i3}}{d_{i2}} \right) = \theta_i,$$

since the arctangent function is strictly increasing. Likewise and under the same conditions, we have that

$$\theta' < 0 \Leftrightarrow \theta > \arctan \left(\frac{d_{i3}}{d_{i2}} \right) = \theta_i$$

and, therefore, we conclude that for $d_{i2} > 0$, the straight line L_i is attractor of surrounding layer dynamics and, therefore, L_i^π is a repeller, as the green part of Figure 8. An analogous study for $d_{i2} < 0$ allows us to reach the results summarized in Table 1.

Table 1: Layer dynamics around the straight lines L_i and L_i^π that compose the slow manifold $\mathcal{M}_i = L_i \cup L_i^\pi$.

| | $d_{i2} < 0$ | $d_{i2} > 0$ |
|-----------|--------------|--------------|
| L_i | repeller | attractor |
| L_i^π | attractor | repeller |

Finally, at $\cos \theta = 0$ with $d_{i2} \neq 0$ the reduced system (27) tells us that $\mathcal{M}_i = \emptyset$ and, therefore, there is only the fast dynamics (28) which reduces to

$$\begin{cases} \dot{x}' = 0 \\ \dot{\theta}' = -d_{i2} \end{cases} \quad \text{and} \quad \begin{cases} \dot{x}' = 0 \\ \dot{\theta}' = d_{i2} \end{cases}$$

for $\theta = \frac{\pi}{2}$ and $\theta = \frac{3\pi}{2}$, respectively, whose dynamics is consistent with Table 1. This completes the qualitative analysis of the layer dynamics and, therefore, the qualitative analysis of this case. See Example 5.1.

5.2 Case $d_{i2} = 0$

Now, the reduced system (27) can be written as

$$\begin{cases} \dot{x} = d_{i1} \\ 0 = d_{i3} \cos \theta \end{cases}, \quad (30)$$

whose slow manifold \mathcal{M}_i is implicitly given by the equation $0 = d_{i3} \cos \theta$ which actually means $0 = \cos \theta$, since we are under (WFH) and, therefore, $d_{i3} \neq 0$. In other words, $\mathcal{M}_i = L_i \cup L_i^\pi$ with L_i and L_i^π being the straight lines given by $\theta = \frac{\pi}{2}$ and $\theta = \frac{3\pi}{2}$, respectively.⁵ The dynamics over and around \mathcal{M}_i behaves exactly as in the case $d_{i2} \neq 0$, but exchanging d_{i2} with d_{i3} at Table 1.

⁴ In particular, when $d_{i3} = 0$ we have $\theta_i = 0$ and, therefore, the straight lines L_i and L_i^π are given by $\theta = 0$ and $\theta = \pi$, respectively, which are part of the stripes' boundary.

⁵ Here, again, the straight lines L_i and L_i^π are part of the boundary of the stripes.

5.3 Theorem and Examples

Summarizing, we conclude that the dynamics over Σ_x for constant fields behaves as described in the theorem below, whose proof consists in the analysis done above in Sections 5.1 and 5.2.

Theorem 5.1 (Constant Dynamics) *Given $\mathbf{F} \in C_3$ with constant components $\mathbf{F}_i = (d_{i1}, d_{i2}, d_{i3})$ such that $d_{i2} \neq 0$ or $d_{i3} \neq 0$, let $\tilde{\mathbf{F}} \in \tilde{C}_3$ be the vector field induced by the blow-up $\phi_1(x, \theta, r) = (x, r \cos \theta, r \sin \theta)$. Then, this blow-up associates the dynamics over Σ_x with the following fundamental dynamics over the cylinder $C = \mathbb{R} \times S^1 = S_1 \cup \dots \cup S_4$: over each stripe S_i acts a slow-fast dynamics whose slow manifold is given by $\mathcal{M}_i = L_i \cup L_i^\pi$, where L_i^π is a π -translation of L_i in θ and*

1. case $d_{i2} \neq 0$, then

$$L_i = \left\{ (x, \theta) \in \mathbb{R} \times [0, 2\pi]; \theta = \arctan\left(\frac{d_{i3}}{d_{i2}}\right) \right\};$$

2. case $d_{i2} = 0$ and $d_{i3} \neq 0$, then

$$L_i = \left\{ (x, \theta) \in \mathbb{R} \times [0, 2\pi]; \theta = \frac{\pi}{2} \right\};$$

which, in both cases, consists of two straight lines inside the cylinder C , possibly invisible relative to S_i . Over this straight lines acts the reduced dynamics $\dot{x} = d_{i1}$ and, around them, acts the layer dynamics described in Table 1, but exchanging d_{i2} with d_{i3} if $d_{i2} = 0$.

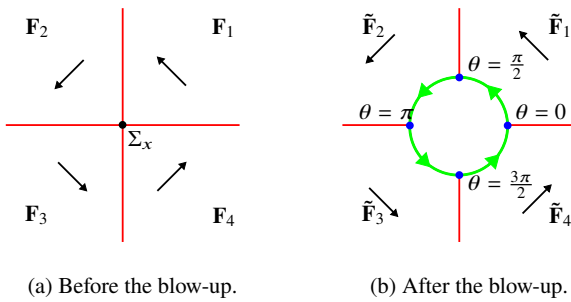


Fig. 9: Slices of the system studied at Example 5.1.

Example 5.1 Let $\mathbf{F} \in C_3$ be given by the constant vector fields

$$\begin{aligned} \mathbf{F}_2(x, y, z) &= (1, -1, -1), & \mathbf{F}_1(x, y, z) &= (1, -1, 1), \\ \mathbf{F}_3(x, y, z) &= (1, 1, -1), & \mathbf{F}_4(x, y, z) &= (1, 1, 1), \end{aligned}$$

that behaves as represented at Figure 9a. Using Theorem 5.1 we can verify that, over the cylinder C given by the blow-up of Σ_x , this system behaves as expected, i.e., as represented at Figure 9b.

For instance, over the stripe $S_1 = \mathbb{R} \times [0, \pi/2]$ we have

$$(d_{11}, d_{12}, d_{13}) = \mathbf{F}_1(x, y, z) = (1, -1, 1)$$

such that, according to Theorem 5.1, induces over S_1 a slow-fast system with $L_1 \subset \mathcal{M}_1$ given by

$$\theta = \theta_1 = \arctan\left(\frac{d_{13}}{d_{12}}\right) = \arctan\left(\frac{1}{-1}\right) = -\frac{\pi}{4},$$

and, therefore, the slow manifold \mathcal{M}_1 consists of the straight lines $L_1 \subset S_4$ and $L_1^\pi \subset S_2$ given by $\theta = \theta_1 = -\frac{\pi}{4}$ and $\theta = \theta_1 + \pi = \frac{3\pi}{4}$, respectively. In particular, none of these lines are visible at S_1 . Over these lines acts the reduced dynamics $\dot{x} = d_{11} = 1$. Finally, since $d_{12} = -1 < 0$, then L_1 is repeller and L_1^π is attractor of surrounding layer dynamics, according to Table 1.

Therefore, we conclude that the dynamics generated by \mathbf{F}_1 over the whole cylinder C behaves as represented in Figure 10. In particular, the dynamics over the stripe S_1 behaves as represented in Figure 9b. The dynamics over the other stripes can be similarly verified to be as represented. \square

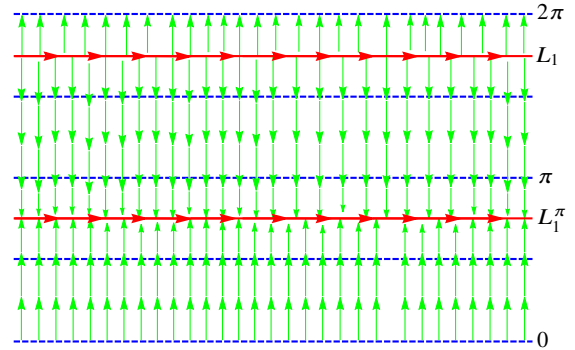


Fig. 10: Dynamics over C generated by the field \mathbf{F}_1 studied at Example 5.1. The dynamics over S_1 behaves as represented in Figure 9b.

6 Affine Dynamics

Let $\mathcal{A}_3 \subset \mathcal{D}_3^k$ be the set of all piecewise smooth vector fields \mathbf{F} with a double discontinuity given by the affine vector fields

$$\begin{aligned} \mathbf{F}_i(x, y, z) &= (a_{i1}x + b_{i1}y + c_{i1}z + d_{i1}, \\ & a_{i2}x + b_{i2}y + c_{i2}z + d_{i2}, \\ & a_{i3}x + b_{i3}y + c_{i3}z + d_{i3}), \end{aligned} \quad (31)$$

where $a_{ij}, b_{ij}, c_{ij}, d_{ij} \in \mathbb{R}$ for all i and j . According to the Fundamental Lemma 4.1, the dynamics over Σ_x of such a field is blow-up associated to the following fundamental dynamics over the cylinder $C = \mathbb{R} \times S^1 = S_1 \cup \dots \cup S_4$: over each stripe S_i acts a slow-fast dynamics whose reduced dynamics is given by

$$\begin{cases} \dot{x} = a_{i1}x + d_{i1} \\ 0 = (a_{i3}x + d_{i3}) \cos \theta - (a_{i2}x + d_{i2}) \sin \theta \end{cases} \quad (32)$$

with radial slow dynamics $\dot{r} = (a_{i2}x + d_{i2}) \cos \theta + (a_{i3}x + d_{i3}) \sin \theta$; and layer dynamics given by

$$\begin{cases} x' = 0 \\ \theta' = (a_{i3}x + d_{i3}) \cos \theta - (a_{i2}x + d_{i2}) \sin \theta \end{cases} \quad (33)$$

with radial fast dynamics $r' = 0$.

Besides that, for (31), we have $p_i = a_{i2}x + d_{i2}$ and $q_i = a_{i3}x + d_{i3}$ so that (WFH) is satisfied as long as

$$a_{i2}x + d_{i2} \neq 0 \quad \text{or} \quad a_{i3}x + d_{i3} \neq 0, \quad (34)$$

whereas, since $(p_i)_x = a_{i2}$ and $(q_i)_x = a_{i3}$, then (SFH) is satisfied as long as

$$\begin{aligned} 0 &\neq p_i(q_i)_x - q_i(p_i)_x = \\ &= (a_{i2}x + d_{i2})a_{i3} - (a_{i3}x + d_{i3})a_{i2} = \\ &= a_{i3}d_{i2} - a_{i2}d_{i3} =: \gamma_i, \end{aligned} \quad (35)$$

which not only assures the fundamental hypothesis but also avoids the already studied constant case, as we will see below.

As in the constant case, our goal at this section is to fully describe the fundamental dynamics of (31) over the cylinder C under the hypothesis (35). In order to do so, we are going to systematically analyze the slow-fast systems (32)–(33) for the cases suggested by (34) and outlined at Table 2.

Table 2: Division (31) dynamics in study cases.

| | $a_{i2}x + d_{i2} \neq 0$ | $a_{i2}x + d_{i2} = 0$ |
|-----------------|---------------------------|------------------------|
| $a_{i2} \neq 0$ | A | B |
| $a_{i2} = 0$ | C | D |

Observe that case (B) actually complements case (A). Moreover, observe that at case (D) we have $a_{i2} = 0$ and $d_{i2} = 0$ which implies the absurd $\gamma_i = 0$. Therefore, cases (A) and (B) complement each other and it will be studied at Section 6.1; case (C) will be studied at Section 6.2. The resulting Theorem 6.1 is stated and exemplified at Section 6.3.

6.1 Case $a_{i2} \neq 0$

Lets start with case (A), i.e., assume that $a_{i2} \neq 0$ and $a_{i2}x + d_{i2} \neq 0$. In order to explicitly define \mathcal{M}_i , observe that whenever $\cos \theta \neq 0$ the second equation of (32) gives us

$$\begin{aligned} 0 &= (a_{i3}x + d_{i3}) \cos \theta - (a_{i2}x + d_{i2}) \sin \theta \Leftrightarrow \\ &\Leftrightarrow \tan \theta = \frac{a_{i3}x + d_{i3}}{a_{i2}x + d_{i2}} =: h(x) \Leftrightarrow \\ &\Leftrightarrow \theta = \arctan \left(\frac{a_{i3}x + d_{i3}}{a_{i2}x + d_{i2}} \right) + n\pi = \theta_i(x) + n\pi, \end{aligned}$$

where $n \in \mathbb{Z}$. As in the constant case, since the subjacent vector fields, (31), are defined for every point of \mathbb{R}^3 , then we can consider \mathcal{M}_i as a subset of the whole cylinder C , not restricted to the particular stripe S_i . Therefore, without loss of generality, the slow manifold can be written as $\mathcal{M}_i = H_i \cup H_i^\pi$, where

$$\begin{aligned} H_i &= \{(x, \theta) \in \mathbb{R} \times [0, 2\pi] ; \theta = \theta_i(x)\} \text{ and} \\ H_i^\pi &= \{(x, \theta) \in \mathbb{R} \times [0, 2\pi] ; \theta = \theta_i(x) + \pi\}, \end{aligned}$$

which consists of two arctangent-normalized hyperboles inside the cylinder $C = \mathbb{R} \times S^1$. In fact, since $a_{i2} \neq 0$, then $h(x)$ is a hyperbole such that

$$\begin{aligned} \frac{d}{dx} h(x) &= \frac{d}{dx} \left[\frac{a_{i3}x + d_{i3}}{a_{i2}x + d_{i2}} \right] = \frac{a_{i3}d_{i2} - d_{i3}a_{i2}}{(a_{i2}x + d_{i2})^2} = \\ &= \frac{\gamma_i}{(a_{i2}x + d_{i2})^2} \end{aligned}$$

or, in other words, it is an increasing hyperbole if $\gamma_i > 0$ and decreasing if $\gamma_i < 0$ ⁶.

Besides that, observe that $h(x)$ has a vertical asymptote at

$$a_{i2}x + d_{i2} = 0 \Leftrightarrow x = -\frac{d_{i2}}{a_{i2}} =: \alpha_i$$

which satisfies

$$\lim_{x \rightarrow \alpha_i^\pm} h(x) = \mp\infty \quad \text{and} \quad \lim_{x \rightarrow \alpha_i^\pm} h(x) = \pm\infty$$

if $\gamma_i > 0$ and $\gamma_i < 0$, respectively; and $h(x)$ has a horizontal asymptote at

$$\lim_{x \rightarrow \pm\infty} h(x) = \lim_{x \rightarrow \pm\infty} \left(\frac{a_{i3}x + d_{i3}}{a_{i2}x + d_{i2}} \right) = \frac{a_{i3}}{a_{i2}}.$$

Translating the information above about the hyperbole $h(x)$ to the arctangent-normalized hyperbole H_i , we get that it

⁶ If $\gamma_i = 0$, then $h(x)$ is a constant function and, therefore, H_i and H_i^π are straight lines. In other words, the constant case is recovered.

- is an increasing curve if $\gamma_i > 0$ and decreasing if $\gamma_i < 0$;
- has a vertical asymptote at $x = \alpha_i$ which satisfies

$$\lim_{x \rightarrow \alpha_i^+} \theta_i(x) = \mp \frac{\pi}{2} \quad \text{and} \quad \lim_{x \rightarrow \alpha_i^-} \theta_i(x) = \pm \frac{\pi}{2}$$

if $\gamma_i > 0$ and $\gamma_i < 0$, respectively;

- has a horizontal asymptote at $\theta = \arctan\left(\frac{a_{i3}}{a_{i2}}\right) =: \beta_i$.

More precisely, the hyperbole H_i behave as the red part of Figure 11a. However, putting together the hyperboles H_i and H_i^π we get that they actually behave as two arctangent-like curves as represented at Figure 11b.

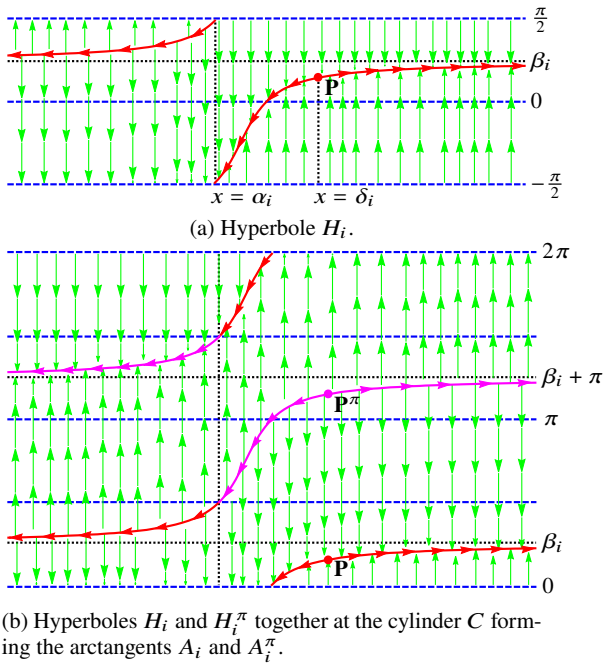


Fig. 11: Affine double discontinuity dynamics for $a_{i1} = 1$, $d_{i1} = -1$, $a_{i2} = 1$, $d_{i2} = 1$, $a_{i3} = 1$ and $d_{i3} = 0$. At this example we have $\alpha_i = -1$, $\beta_i = \frac{\pi}{4}$ and $\delta_i = 1$. Therefore, for example, S_1 has part of the hyperbole H_i as a visible part of the slow manifold; whereas S_2 has only part of A_i^π visible.

These arctangent-like curves will be denoted by A_i and A_i^π . Based on the analysis done before, we conclude that they are given by

$$\begin{aligned} A_i &= \{(x, \theta) \in [-\infty, \alpha_i] \times [0, 2\pi]; \theta = \theta_i(x) + \pi\} \cup \\ &\quad \cup \{(x, \theta) \in [\alpha_i, +\infty] \times [0, 2\pi]; \theta = \theta_i(x)\}, \\ A_i^\pi &= \{(x, \theta) \in [-\infty, \alpha_i] \times [0, 2\pi]; \theta = \theta_i(x)\} \cup \\ &\quad \cup \{(x, \theta) \in [\alpha_i, +\infty] \times [0, 2\pi]; \theta = \theta_i(x) + \pi\}, \end{aligned}$$

and, therefore, on one hand, A_i is an arctangent-like curve with $\theta = \beta_i + \pi$ and $\theta = \beta_i$ as negative and positive⁷ hor-

izontal asymptotes, respectively; on the other hand, A_i^π is an arctangent-like curve with $\theta = \beta_i$ and $\theta = \beta_i + \pi$ as negative and positive horizontal asymptotes, respectively.⁸ Moreover, because of the very definition of β_i , the positioning of the asymptotes inside the cylinder behaves similarly as the straight lines L_i and L_i^π in Section 5. This completes the qualitative analysis of the shape of the slow manifold and, from now on we will write $\mathcal{M}_i = A_i \cup A_i^\pi$.

Over both the arctangents $\mathcal{M}_i = A_i \cup A_i^\pi$, we have the one-dimensional dynamics given by the first equation of (32), i.e., $\dot{x} = a_{i1}x + d_{i1}$. Analyzing this equation we observe that, if $a_{i1} \neq 0$, then there are hyperbolic critical points at

$$x = -\frac{d_{i1}}{a_{i1}} =: \delta_i,$$

being these points attractors if $a_{i1} < 0$ and repellers if $a_{i1} > 0$, as represented at Figure 11b. Since we are under (SFH), then Theorem 4.5 tells us that, in this case, these hyperbolic singularities are actually hyperbolic singularities of the whole stripe S_i . If $a_{i1} = 0$, then there is no critical point and the dynamics over \mathcal{M}_i is exactly as in the constant case described in Section 5. This completes the qualitative analysis of the reduced dynamics.

Regarding the layer dynamics, we have the layer system (33) which says that for each fixed value of $x \in \mathbb{R}$, we have a one-dimensional dynamics given by the second equation of (33). In particular, assuming that $\cos \theta > 0$ and $a_{i2}x + d_{i2} > 0$, then

$$\theta' > 0 \Leftrightarrow \theta < \theta_i(x),$$

since the arctangent function is strictly increasing. Likewise, and under the same conditions, we have that

$$\theta' < 0 \Leftrightarrow \theta > \theta_i(x),$$

and, therefore, we conclude that for $a_{i2}x + d_{i2} > 0$, the piece of curve $\theta = \theta_i(x)$ is attractor of the surrounding dynamics and, therefore, $\theta = \theta_i(x) + \pi$ is repeller. Moreover, if $a_{i2} > 0$, then $a_{i2}x + d_{i2} > 0$ happens for $x > \alpha_i$; if $a_{i2} < 0$, then $a_{i2}x + d_{i2} > 0$ happens for $x < \alpha_i$. Completing this analysis and comparing with the definition of A_i and A_i^π we reach the results summarized at Table 3 and represented as the green part of Figure 11. Moreover, at $\cos \theta = 0$ with $a_{i2} \neq 0$ and $a_{i2}x + d_{i2} \neq 0$, (33) give us the layer systems

$$\begin{cases} x' = 0 \\ \theta' = -(a_{i2}x + d_{i2}) \end{cases} \quad \text{and} \quad \begin{cases} x' = 0 \\ \theta' = a_{i2}x + d_{i2} \end{cases}$$

⁸ In particular, when $a_{i3} = 0$ we have $\beta_i = 0$ and, therefore, the horizontal asymptotes are given by $\theta = 0$ and $\theta = \pi$, which are part of the stripes' boundary.

⁷ Where negative means $x \rightarrow -\infty$ and positive means $x \rightarrow +\infty$.

for $\theta = \frac{\pi}{2}$ and $\theta = \frac{3\pi}{2}$, respectively, whose dynamics is consistent with Table 3. This completes the qualitative analysis of the layer dynamics for case (A).

Now, let's consider the case (B), which complements the case (A) studied above defining the missing dynamics over $a_{i2}x + d_{i2} = 0$ ($\Leftrightarrow x = \alpha_i$) with $a_{i2} \neq 0$. At this case, the reduced system (32) becomes

$$\begin{cases} \dot{x} = a_{i1}x + d_{i1} \\ 0 = (a_{i3}x + d_{i3}) \cos \theta \end{cases}$$

whose slow manifold \mathcal{M}_i is implicitly given by the equation $0 = (a_{i3}x + d_{i3}) \cos \theta$ which actually means $0 = \cos \theta$, since we are under SFH and, therefore $a_{i3}x + d_{i3} \neq 0$. In other words, $\mathcal{M}_i = \left\{ \left(\alpha_i, \frac{\pi}{2} \right), \left(\alpha_i, \frac{3\pi}{2} \right) \right\}$. Over these points acts the dynamics $\dot{x} = a_{i1}x + d_{i1}$, which is consistent with case (A). Regarding the fast dynamics, we have the layer system

$$\begin{cases} x' = 0 \\ \theta' = (a_{i3}x + d_{i3}) \cos \theta \end{cases} \sim \begin{cases} x' = 0 \\ \theta' = -\frac{\gamma_i}{a_{i2}} \cos \theta \end{cases}$$

since $x = \alpha_i$, which can be easily verified to be consistent with the layer dynamics given by Table 3 and, therefore, it is consistent with case (A). Therefore, we conclude that case whole (B) is consistent with case (A). In other words, the dynamics over the asymptote $a_{i2}x + d_{i2} = 0$ agrees with the surrounding dynamics.

Table 3: Layer dynamics around the arctangents A_i and A_i^π that compose the slow manifold $\mathcal{M}_i = A_i \cup A_i^\pi$.

| | $a_{i2} < 0$ | $a_{i2} > 0$ |
|-----------|--------------|--------------|
| A_i | repellor | attractor |
| A_i^π | attractor | repellor |

6.2 Case $a_{i2} = 0$

For case (C), remember that we have $a_{i2} = 0$ and $a_{i2}x + d_{i2} \neq 0$ implying $d_{i2} \neq 0$. Therefore, everything at the beginning of Section 6.1 is true. However, whenever $\cos \theta \neq 0$, the explicit expression for the slow manifold \mathcal{M}_i is now

$$\theta = \arctan\left(\frac{a_{i3}x + d_{i3}}{d_{i2}}\right) + n\pi = \theta_i(x) + n\pi,$$

where $n \in \mathbb{Z}$. Therefore, without loss of generality, the slow manifold can be written as $\mathcal{M}_i = A_i \cup A_i^\pi$, where

$$\begin{aligned} A_i &= \{(x, \theta) \in \mathbb{R} \times [0, 2\pi]; \theta = \theta_i(x)\} \text{ and} \\ A_i^\pi &= \{(x, \theta) \in \mathbb{R} \times [0, 2\pi]; \theta = \theta_i(x) + \pi\}, \end{aligned}$$

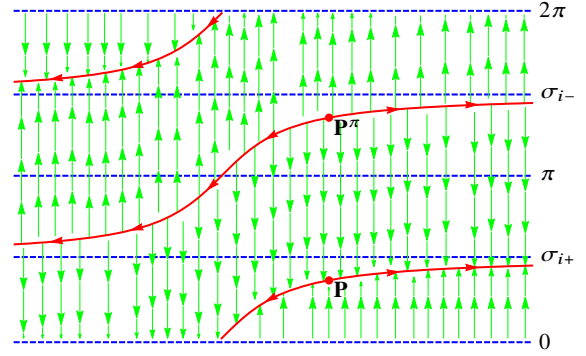


Fig. 12: Affine double discontinuity dynamics for $a_{i1} = 1$, $d_{i1} = -1$, $a_{i2} = 0$, $d_{i2} = 1$, $a_{i3} = 1$ and $d_{i3} = 1$. At this example we have $\delta_i = 1$ and $\sigma_{i\pm} = \pm \frac{\pi}{2}$.

which consists of two arctangent-like curves inside the cylinder $C = \mathbb{R} \times S^1$ as the red part of Figure 12. In fact, since $a_{i2} = 0$, then $h(x)$ is a straight line and, therefore,

$$\theta = \theta_i(x) = \arctan(h(x))$$

is an arctangent curve. Besides that, we have

$$\frac{d}{dx} h(x) = \frac{\gamma_i}{(a_{i2}x + d_{i2})^2} = \frac{\gamma_i}{d_{i2}^2}$$

and, therefore, A_i and A_i^π are increasing curves if $\gamma_i > 0$ and decreasing if $\gamma_i < 0$ ⁹. Moreover, since

$$\begin{aligned} \lim_{x \rightarrow \pm\infty} \theta_i(x) &= \lim_{x \rightarrow \pm\infty} \left[\arctan\left(\frac{a_{i3}x + d_{i3}}{d_{i2}}\right) \right] = \\ &= \arctan\left[\lim_{x \rightarrow \pm\infty} \left(\frac{a_{i3}x + d_{i3}}{d_{i2}}\right) \right] = \\ &= \arctan\left[\pm \operatorname{sgn}\left(\frac{a_{i3}}{d_{i2}}\right) \infty \right] = \\ &= \pm \operatorname{sgn}\left(\frac{a_{i3}}{d_{i2}}\right) \frac{\pi}{2} = \pm \operatorname{sgn}\left(\frac{\gamma_i}{d_{i2}^2}\right) \frac{\pi}{2} = \\ &= \pm \operatorname{sgn}(\gamma_i) \frac{\pi}{2} =: \sigma_{i\pm}, \end{aligned}$$

then A_i has σ_{i-} and σ_{i+} as negative and positive horizontal asymptote, respectively; while A_i^π has σ_{i+} and σ_{i-} as negative and positive horizontal asymptote, respectively. This completes the qualitative analysis of the shape of the slow manifold.

Over both the arctangents $\mathcal{M}_i = A_i \cup A_i^\pi$, we have the one-dimensional dynamics given by the first equation of (32), i.e., $\dot{x} = a_{i1}x + d_{i1}$ which behaves as described in Section 6.1.

⁹ Again, if $\gamma_i = 0$ ($\Leftrightarrow a_{i3} = 0$), then $h(x)$ is a constant function and, therefore, A_i and A_i^π are straight lines. In other words, the constant case is recovered.

This completes the qualitative analysis of the reduced dynamics.

Regarding the layer dynamics, a completely analogous analysis such as that made for the previous cases allows us to conclude that it behaves as described in Table 3, including the case $\cos \theta = 0$, but exchanging a_{i2} with d_{i2} .

6.3 Theorem and Examples

Summarizing, we conclude that the dynamics over Σ_x for affine fields behaves as described in the theorem below, whose proof consists in the analysis done above.

Theorem 6.1 (Affine Dynamics) *Given $\mathbf{F} \in \mathcal{A}_3$ with affine components \mathbf{F}_i given by (31) and such that $\gamma_i \neq 0$, let $\tilde{\mathbf{F}} \in \tilde{\mathcal{A}}_3$ be the vector field induced by the blow-up $\phi_1(x, \theta, r) = (x, r \cos \theta, r \sin \theta)$. Then, this blow-up associates the dynamics over Σ_x with the following fundamental dynamics over the cylinder $C = \mathbb{R} \times S^1 = S_1 \cup \dots \cup S_4$: over each stripe S_i acts a slow-fast dynamics whose slow manifold is given by $\mathcal{M}_i = A_i \cup A_i^\pi$, where A_i^π is a π -translation of A_i in θ and*

1. case $a_{i2} \neq 0$, then

$$A_i = \{(x, \theta) \in [-\infty, \alpha_i] \times [0, 2\pi]; \theta = \theta_i(x) + \pi\} \cup \{(x, \theta) \in [\alpha_i, +\infty] \times [0, 2\pi]; \theta = \theta_i(x)\}$$

with $\theta_i(x) = \arctan\left(\frac{a_{i3}x + d_{i3}}{a_{i2}x + d_{i2}}\right)$, which consists of an arctangent-like curve inside the cylinder C with $\theta = \beta_i + \pi$ and $\theta = \beta_i$ as negative and positive horizontal asymptotes, respectively;

2. case $a_{i2} = 0$, then

$$A_i = \{(x, \theta) \in \mathbb{R} \times [0, 2\pi]; \theta = \theta_i(x)\}$$

with $\theta_i(x) = \arctan\left(\frac{a_{i3}x + d_{i3}}{d_{i2}}\right)$, which consists of an arctangent-like curve inside the cylinder C with $\theta = \sigma_{i-}$ and $\theta = \sigma_{i+}$ as negative and positive horizontal asymptotes, respectively.

Both arctangents are increasing if $\gamma_i > 0$ and decreasing if $\gamma_i < 0$. Over them act the reduced dynamics $\dot{x} = a_{i1}x + d_{i1}$ and, around them, acts the layer dynamics described in Table 3, but exchanging a_{i2} with d_{i2} if $a_{i2} = 0$. Finally, the new parameters above are given by $\alpha_i = -\frac{d_{i2}}{a_{i2}}$, $\beta_i = \arctan\left(\frac{a_{i3}}{a_{i2}}\right)$, $\gamma_i = a_{i3}d_{i2} - d_{i3}a_{i2}$, $\delta_i = -\frac{d_{i1}}{a_{i1}}$ and $\sigma_{i\pm} = \pm \operatorname{sgn}(\gamma_i) \frac{\pi}{2}$.

Example 6.1 Let $\mathbf{F} \in \mathcal{A}_3$ be given by affine vector fields such that

$$\mathbf{F}_2 : \begin{bmatrix} a_{21} & d_{21} \\ a_{22} & d_{22} \\ a_{23} & d_{23} \end{bmatrix} = \begin{bmatrix} 1 & -2 \\ -1 & 1 \\ -1 & 0 \end{bmatrix}, \quad \mathbf{F}_1 : \begin{bmatrix} a_{11} & d_{11} \\ a_{12} & d_{12} \\ a_{13} & d_{13} \end{bmatrix} = \begin{bmatrix} -1 & 2 \\ -1 & 1 \\ 1 & 0 \end{bmatrix},$$

$$\mathbf{F}_3 : \begin{bmatrix} a_{31} & d_{31} \\ a_{32} & d_{32} \\ a_{33} & d_{33} \end{bmatrix} = \begin{bmatrix} 1 & -2 \\ 1 & 1 \\ -1 & 0 \end{bmatrix}, \quad \mathbf{F}_4 : \begin{bmatrix} a_{41} & d_{41} \\ a_{42} & d_{42} \\ a_{43} & d_{43} \end{bmatrix} = \begin{bmatrix} -1 & 2 \\ 1 & 1 \\ 1 & 0 \end{bmatrix},$$

with parameters c_{ij} 's and d_{ij} 's arbitrary since, according to Theorem 6.1, they only affect the dynamics outside the cylinder. Using this theorem we can also verify that, over the cylinder C given by the blow-up of Σ_x , the system has a single **slow cycle** as represented at Figure 13.

For instance, according to Theorem 6.1, the field \mathbf{F}_1 induces a slow-fast system whose slow manifold $\mathcal{M}_1 = A_1 \cup A_1^\pi$ consists of arctangents with horizontal asymptotes

$$\theta = \beta_1 = \arctan\left(\frac{a_{13}}{a_{12}}\right) = \arctan(-1) = -\frac{\pi}{4}$$

at S_4 and $\theta = \beta_1 + \pi = \frac{3\pi}{4}$ at S_2 . Besides that, since

$$\gamma_1 = a_{13}d_{12} - a_{12}d_{13} = 1$$

then these arctangents are increasing. Therefore, we conclude that $\mathcal{M}_1 \cap S_1 \subset A_1^\pi$, and it transversally crosses S_1 as represented at the lowest stripe of Figure 13 from \mathbf{R}_1 to \mathbf{Q}_1 , where the point \mathbf{Q}_1 is given by

$$\frac{\pi}{2} = \theta_1(x) = \arctan\left(\frac{a_{13}x + d_{13}}{a_{12}x + d_{12}}\right) = \arctan\left(\frac{x}{-x + 1}\right),$$

which happens when $x \rightarrow 1^-$; and the point \mathbf{R}_1 is given by

$$0 = \theta_1(x) = \arctan\left(\frac{a_{13}x + d_{13}}{a_{12}x + d_{12}}\right) = \arctan\left(\frac{x}{-x + 1}\right),$$

which happens when $x \rightarrow 0^+$. Dynamically it also goes $\mathbf{R}_1 \rightarrow \mathbf{Q}_1$, since over $\mathcal{M}_1 \cap S_1$ acts the reduced dynamics $\dot{x} = -x + 2$, which has $x = 2$ as a stable singularity. Finally, since $a_{12} = -1 < 0$ and $\mathcal{M}_1 \cap S_1 \subset A_1^\pi$, then $\mathcal{M}_1 \cap S_1$ attracts the surrounding layer dynamics, according to Table 3.

Therefore, we conclude that the dynamics generated by \mathbf{F}_1 over the stripe S_1 , in fact, behave as represented at Figure 13. The dynamics over the other stripes can be similarly verified to be as represented. \square

Corollary 6.1 *Every $\mathbf{F} \in \mathcal{A}_3$ with $\gamma_i \neq 0$ can induce at most one slow cycle over the cylinder.*

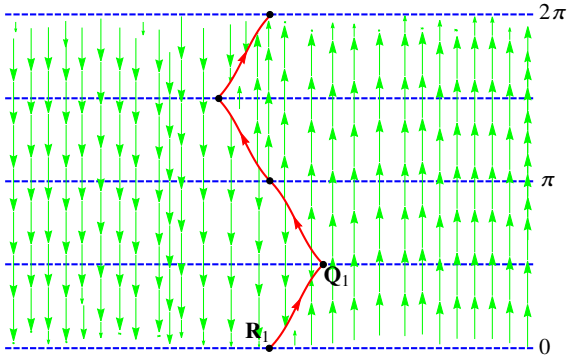


Fig. 13: Dynamics over C generated by the field \mathbf{F} studied at Example 6.1.

Proof Given a stripe S_i , according to Theorem 6.1 the arctangents that forms the slow manifold \mathcal{M}_i can either have a horizontal asymptote inside S_i or not.

If a horizontal asymptote is inside S_i , then a slow cycle construction is impossible, even if the asymptote is at one of the borders of S_i , since \mathcal{M}_i does not cross transversally both borders of S_i .

However, if no horizontal asymptote is inside S_i , then a construction similar to that realized at Example 6.1 can occur. Finally, no more than one slow cycle can occur, since the arctangents are strictly monotonous and, therefore, transversally crosses S_i at most once.

7 Structural Stability

Let $\mathbf{F} \in \mathcal{D}_3^k$ be a piecewise smooth vector field with a double discontinuity given by affine vector fields (31). The theorems obtained in the previous sections fully describe the constant and affine fundamental dynamics over the cylinder C of the induced vector field $\tilde{\mathbf{F}} \in \tilde{\mathcal{D}}_3^k$. As an application, we would like to leverage this knowledge to study its structural stability. The first step in this process consists of defining a concept of structural stability which fits the systems we are studying. In order to do so, we are going to mimic the classical definition for the regular case, $\mathcal{R}^k(U)$, presented in [42, p. 18], which can be easily extended to \mathcal{D}_3^k . In fact, on one hand, systems in $\mathcal{R}^k(U)$ have a single subset that should be kept invariant, $\Sigma = h^{-1}(0)$; on the other hand, systems in \mathcal{D}_3^k have a set of subsets

$$\mathcal{I} = \{\Sigma_{12}, \Sigma_{23}, \Sigma_{34}, \Sigma_{14}, \Sigma_x\}$$

which should be kept invariants by topological equivalence. Therefore, a direct substitution gives us the following definition:

Definition 7.1 Let $\mathbf{F}, \mathbf{G} \in \mathcal{D}_3^k$. We say that \mathbf{F} and \mathbf{G} are **topologically equivalent** and denote $\mathbf{F} \sim \mathbf{G}$ if, and only

if, there exists a homeomorphism $\varphi : \mathbb{R}^3 \rightarrow \mathbb{R}^3$ that keeps every $I \in \mathcal{I}$ invariant and takes orbits of \mathbf{F} into orbits of \mathbf{G} preserving the orientation of time. From this definition the concept of structural stability in \mathcal{D}_3^k is naturally obtained.

For the blow-up induced vector fields, $\tilde{\mathcal{D}}_3^k$, the set of invariant subsets are given by

$$\tilde{\mathcal{I}} = \{\tilde{\Sigma}_{12}, \tilde{\Sigma}_{23}, \tilde{\Sigma}_{34}, \tilde{\Sigma}_{14}, C\}$$

and, therefore, we define:

Definition 7.2 Let $\tilde{\mathbf{F}}, \tilde{\mathbf{G}} \in \tilde{\mathcal{D}}_3^k$. We say that $\tilde{\mathbf{F}}$ and $\tilde{\mathbf{G}}$ are **topologically equivalent** and denote $\tilde{\mathbf{F}} \sim \tilde{\mathbf{G}}$ if, and only if, there exists a homeomorphism $\tilde{\varphi} : \mathbb{R} \times S^1 \times \mathbb{R}^+ \rightarrow \mathbb{R} \times S^1 \times \mathbb{R}^+$ that keeps every $I \in \tilde{\mathcal{I}}$ invariant and takes orbits of $\tilde{\mathbf{F}}$ into orbits of $\tilde{\mathbf{G}}$ preserving the orientation of time. From this definition the concept of structural stability in $\tilde{\mathcal{D}}_3^k$ is naturally obtained.

Now, let $\tilde{\mathbf{F}}, \tilde{\mathbf{G}} \in \tilde{\mathcal{D}}_3^k$ be topologically equivalent by a homeomorphism $\tilde{\varphi}$. In this case, we have that $\tilde{\varphi}|_I$ with $I \in \tilde{\mathcal{I}}$ are also homeomorphisms taking orbits into orbits and preserving the orientation of time. In other words, the existence of these homeomorphisms is a necessary condition for the topological equivalence. More precisely:

Proposition 7.1 If $\tilde{\mathbf{F}} \sim \tilde{\mathbf{G}}$, then $\tilde{\mathbf{F}}|_I \sim \tilde{\mathbf{G}}|_I$ for every $I \in \tilde{\mathcal{I}}$.

We are interested on the dynamics over the cylinder C . Therefore, given $\mathbf{F} \in \mathcal{D}_3^k$, we look for necessary and/or sufficient conditions for the structural stability of $\tilde{\mathbf{F}}|_C$. Beyond the intrinsic interest, given in Proposition 7.1 above, such conditions shall also reveal relevant information on the structural stability of \mathbf{F} and, therefore, on the structural stability of \mathbf{F} . In fact, from Proposition 7.1 it follows the result below.

Corollary 7.1 If $\tilde{\mathbf{F}}$ is structurally stable, then $\tilde{\mathbf{F}}|_I$ is structurally stable for every $I \in \tilde{\mathcal{I}}$.

Proof Given $I \in \tilde{\mathcal{I}}$, let $\tilde{\mathcal{W}} \subset \tilde{\mathcal{D}}_3^k$ be an open neighborhood of $\tilde{\mathbf{F}}$. Observe that

$$\tilde{\mathcal{W}}|_I = \{\tilde{\mathbf{H}}|_I; \tilde{\mathbf{H}} \in \tilde{\mathcal{W}}\}$$

is an open neighborhood of $\tilde{\mathbf{F}}|_I$.

Therefore, if $\tilde{\mathbf{F}}|_I$ was not structurally stable, would exist $\tilde{\mathbf{G}}|_I \in \tilde{\mathcal{W}}|_I$ such that $\tilde{\mathbf{F}}|_I \not\sim \tilde{\mathbf{G}}|_I$ and, therefore, from Proposition 7.1 would follow that $\tilde{\mathbf{G}} \not\sim \tilde{\mathbf{F}}$, then implying that $\tilde{\mathbf{F}}$ would not be structurally stable.

Thus, from now on, we will exclusively study conditions for the structural stability of $\tilde{\mathbf{F}}|_C$. In order to do so, remember that over C acts a regular Filippov dynamics whose switching manifold is formed by the elements of

$$\tilde{\mathcal{I}}_C = \left\{ \Sigma_0, \Sigma_{\frac{\pi}{2}}, \Sigma_{\pi}, \Sigma_{\frac{3\pi}{2}} \right\},$$

where $\Sigma_\theta = \{(x, \theta); x \in \mathbb{R}\}$. Therefore, without loss of generality for the previous results, it is natural to adopt the following definitions of equivalence and stability for C :

Definition 7.3 Let $\tilde{\mathbf{F}}, \tilde{\mathbf{G}} \in \mathcal{D}_3^k$. We say that $\tilde{\mathbf{F}}$ and $\tilde{\mathbf{G}}$ are C -**topologically equivalent** and denote $\tilde{\mathbf{F}} \sim_c \tilde{\mathbf{G}}$ if, and only if, there exists a homeomorphism $\tilde{\varphi} : C \rightarrow C$ that keeps every $I \in \tilde{\mathcal{I}}_C$ invariant and takes orbits of $\tilde{\mathbf{F}}|_C$ into orbits of $\tilde{\mathbf{G}}|_C$ preserving the orientation of time. From this definition the concept of C -structural stability is naturally obtained.

Although global and naturally derived from the regular case, C -structural stability, as presented above, is still a fairly complex property to prove and, in fact, to the best of the author's knowledge, it is an open problem to characterize it through simple conditions and, therefore, shall be treated in future works.

However, many of the difficulties found at characterizing C -structural stability comes from its global aspect. In fact, conditions for a semi-local approach can be found in [7] and, in order to apply these results, a *regular* and *compact* Filippov section of the cylinder C must be taken.

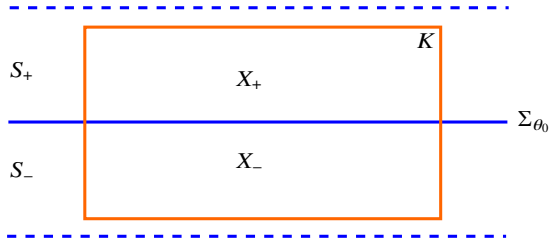


Fig. 14: Regular Filippov system $\mathbf{X} = (\mathbf{X}_-, \mathbf{X}_+)$ defined at a convex compact set $K \subset C_+ \cup C_-$ with switching manifold Σ_{θ_0} .

More precisely, given $\mathbf{F} \in \mathcal{D}_3^k$ and two consecutive stripes C_+ and C_- meeting at a straight line $\Sigma_{\theta_0} \in \tilde{\mathcal{I}}_C$, let \mathbf{X}_+ and \mathbf{X}_- be the smooth vector fields induced over $C_+ \cap K$ and $C_- \cap K$, respectively, as described at the previous sections and where $K \subset C_+ \cup C_-$ is a convex compact set, see Figure 14. Observe that $\mathbf{X} = (\mathbf{X}_-, \mathbf{X}_+)$ is a *regular* and *compact* Filippov system with a connected (due to the convexity of K) switching manifold Σ_{θ_0} .

Then, a direct application of Theorem B from [7, p. 5] and the Proposition 1.1 from [35, p. 122] give us the following result:

Proposition 7.2 Given $\mathbf{F} \in \mathcal{D}_3^k$, two consecutive stripes C_+ and C_- and a convex compact set $K \subset C_+ \cup C_-$, then the

induced Filippov system $\mathbf{X} = (\mathbf{X}_-, \mathbf{X}_+)$ is structurally stable inside K if, and only if, the following sets of conditions are satisfied:

- (I) \mathbf{X}_+ and \mathbf{X}_- are robustly¹⁰ Morse-Smale, i.e., they have:
 - (C.1) finitely many critical elements¹¹, all hyperbolic;
 - (C.2) no saddle-connections;
 - (C.3) only critical elements as non-wandering points;
- (II) \mathbf{X}_+ and \mathbf{X}_- robustly satisfies that:
 - (C.4) none of them vanishes at a point of Σ_{θ_0} ;
 - (C.5) they are tangent to Σ_{θ_0} at only finitely many points with both never tangent at the same point;
 - (C.6) they are colinear at only finitely many points;
- (III) \mathbf{X} have:
 - (C.7) only hyperbolic periodic orbits;
 - (C.8) no separatrix-connections or relations¹²;
 - (C.9) only trivial recurrent orbits.

Observe that (I) refers only to the usual dynamics of \mathbf{X}_+ and \mathbf{X}_- over the smooth parts. On the other hand, (II) considers only the values of \mathbf{X}_+ and \mathbf{X}_- over the switching manifold Σ_{θ_0} . Finally, only (III) refers to the actual Filippov dynamics of \mathbf{X} . With that in mind, over the next, and final sections, we will apply Theorem 5.1 and Theorem 6.1 to analyze this conditions for the particular cases of constant and affine double discontinuities, respectively, and therefore derive semi-local structural stability theorems or, more precisely:

Definition 7.4 We say that $\mathbf{F} \in \mathcal{D}_3^k$ is (I, K) -**semi-local structurally stable** if, and only if, the induced Filippov system $\mathbf{X} = (\mathbf{X}_-, \mathbf{X}_+)$ is structurally stable inside a convex compact set $K \subset C_+ \cup C_-$, where C_+ and C_- are two consecutive stripes meeting at $I \in \tilde{\mathcal{I}}_C$.

In fact, given the bifurcation described below, it is natural to study the constant and affine cases separately, since the first is always structurally unstable inside the last one. More precisely:

Proposition 7.3 Every $\mathbf{F} \in \mathcal{C}_3$ is structurally unstable as an element of \mathcal{A}_3 .

Proof Let $\mathbf{F} \in \mathcal{C}_3 \subset \mathcal{D}_3^k$ be a piecewise smooth vector field with a double discontinuity given by constant vector fields

$$\mathbf{F}_i(x, y, z) = (d_{i1}, d_{i2}, d_{i3}),$$

where $d_{ij} \in \mathbb{R}$ for all i and j .

Assume, without loss of generality, that $d_{i1} > 0$. Then, according to Theorem 5.1, over the slow manifold we have

¹⁰ In other words, the property is stable under small perturbations.

¹¹ Singularities and periodic orbits.

¹² Unstable separatrices arriving at the same point are said to be **related**.

the dynamics $\dot{x} = d_{i1}$. As $d_{i1} > 0$, then it is strictly increasing and, in particular, has no singularities.

However, considering \mathbf{F} as an element of $\mathcal{A}_3 \subset \mathcal{D}_3^k$ and, in particular, perturbing \mathbf{F}_i inside \mathcal{A}_3 with $a_{i1} \neq 0$, then we would now have the dynamics $\dot{x} = a_{i1}x + d_{i1}$ over the slow manifold. As $d_{i1} > 0$ and $a_{i1} \neq 0$, then it does now have a single singularity at $x = \delta_i$ and, besides that, half of its stability was inverted when compared with the unperturbed dynamics.

In other words, \mathbf{F} as an element of \mathcal{A}_3 violates the robustness of condition (C.1) of Proposition 7.2 and, therefore, is structurally unstable.

7.1 Constant Dynamics

Let $\mathbf{F} \in \mathcal{C}_3$ be a piecewise smooth vector field with a double discontinuity given by constant vector fields

$$\mathbf{F}_i(x, y, z) = (d_{i1}, d_{i2}, d_{i3}), \quad (36)$$

with $d_{i2} \neq 0$ or $d_{i3} \neq 0$. Remember that, in this case, Theorem 5.1 provides a full description of the fundamental dynamics of (36) and, therefore, we would like to combine it with Proposition 7.2 to derive a semi-local structural stability theorem.

In order to apply this results, given $\Sigma_{\theta_0} \in \tilde{\mathcal{I}}_C$, let $\mathbf{X} = (\mathbf{X}_-, \mathbf{X}_+)$ be the Filippov system induced by (36) in a convex compact set $K \subset C_+ \cup C_-$, where C_+ and C_- are two consecutive stripes meeting at Σ_{θ_0} as represented at Figure 14. According to Theorem 5.1, the following are the possible categories of dynamics for a stripe $S_i \in \{C_+, C_-\}$, which we now analyze against conditions (C.1) — (C.5) of Proposition 7.2 case by case in order to discover those that can possibly generate structural stable systems, henceforth called **candidates**:

1. $d_{i2} \neq 0$:

(a) $d_{i3} \neq 0$:

One, and only one, of the straight lines L_i or L_i^π is visible inside the stripe. Hence, if $d_{i1} = 0$, then we have a continuum of singularities, i.e., a violation of condition (C.1). However, if $d_{i1} \neq 0$, then no critical elements are present and, therefore (C.1) and (C.2) validates. About (C.3), since the slow manifold acts as α or ω -limit of the surrounding dynamics, then it also validates if $d_{i1} \neq 0$. Even more, since over the borders of S_i there is only transversal layer dynamics, then (C.4) and (C.5) also validates. Finally, observe that, invoking theorems such as *continuity theorems* and *Thom Transversality Theorem*, we easily conclude the robustness of the properties validated above when perturbing inside \mathcal{C}_3 . Therefore, this case is a *candidate* if, and only if, $d_{i1} \neq 0$.

(b) $d_{i3} = 0$:

The only difference between this case and the previous is the fact that, now, one of straight lines L_i or L_i^π is over one of the borders of the stripe S_i and, therefore, (C.5) is possibly violated, whatever d_{i1} . More specifically, if L_i or L_i^π coincides with Σ_{θ_0} , then we have instability; otherwise, we have a *candidate*.

2. $d_{i2} = 0$ and $d_{i3} \neq 0$:

This case is similar to the previous one ($d_{i2} \neq 0$ and $d_{i3} = 0$): whatever d_{i1} , if L_i or L_i^π coincides with Σ_{θ_0} , then we have instability; otherwise, we have a *candidate*.

The analysis of the remaining conditions (C.6) — (C.9) requires the combined dynamics of the stripes C_+ and C_- . Therefore, in order to decide stability, we shall now analyze all the combinations of candidates obtained above, and summarized at Table 4, against these conditions.

Table 4: Conditions under which the stripe S_i is a semi-local structural stability candidate.

| | $d_{i2} \neq 0$ | $d_{i2} = 0$ |
|-----------------|--------------------------|--------------------------|
| $d_{i3} \neq 0$ | $d_{i1} \neq 0$ | $\theta_i \neq \theta_0$ |
| $d_{i3} = 0$ | $\theta_i \neq \theta_0$ | unstable |

Actually, most of the remaining conditions can be easily dropped. In fact, according to Theorem 5.1, none of the candidates have periodic orbits and, besides that, because of the α and ω -limit nature of \mathcal{M}_i , an orbit that enters S_i never touches the same border again and, therefore, (C.7) always validates, because there is no periodic orbits. Likewise, there is no singularities, usual or not and, therefore, there is no separatrix-connections or relations, i.e., (C.8) always validates. Finally, as long as $d_{i1} \neq 0$, Poincaré-Bendixson Theorem assures that no non-trivial recurrent orbits can happen inside S_i and, besides that, again because of the α and ω -limit nature of \mathcal{M}_i , neither can they happen through the switching manifold and, therefore, (C.9) also always validates. At this point, the following theorem has been proved:

Theorem 7.1 (Constant Dynamics Stability) *Let $\mathbf{F} \in \mathcal{C}_3$ be given by (36) with $d_{i2} \neq 0$ or $d_{i3} \neq 0$. Given $\Sigma_{\theta_0} \in \tilde{\mathcal{I}}_C$, let $\mathbf{X} = (\mathbf{X}_-, \mathbf{X}_+)$ be the Filippov system induced around Σ_{θ_0} and inside a convex compact set $K \subset C_+ \cup C_-$, where C_+ and C_- are two consecutive stripes meeting at Σ_{θ_0} . Then, \mathbf{F} is (Σ_{θ_0}, K) -semi-local structurally stable in \mathcal{C}_3 if, and only if, \mathbf{X}_+ and \mathbf{X}_- satisfies at least one of the conditions*

1. $d_{i1}d_{i2}d_{i3} \neq 0$; or
2. $d_{i1} \neq 0$, $d_{i2}^2 + d_{i3}^2 \neq 0$ and $\theta_i \neq \theta_0$;

and, additionally, \mathbf{X}_+ and \mathbf{X}_- are non-colinear over Σ_{θ_0} , except at finitely many points.

Example 7.1 Lets see an example of instability around the discontinuity manifold $\Sigma_{\frac{\pi}{2}} \in \tilde{\mathcal{I}}_C$ of the cylinder generated by constant vector fields. More precisely, take $\mathbf{F} \in \mathcal{C}_3$ with

$$\mathbf{F}_1(x, y, z) = (1, -1, 1) \quad \text{and} \quad \mathbf{F}_2(x, y, z) = (-1, 1, 1),$$

whose dynamics over the stripes $S_1 \cup S_2$, represented at Figure 15 below, can be determined as in Example 5.1 using Theorem 5.1.

Since $d_{11}d_{12}d_{13} = -1 \neq 0$ and $d_{21}d_{22}d_{23} = -1 \neq 0$, then the first part of Theorem 7.1 is satisfied. However, the induced dynamics \mathbf{X}_1 and \mathbf{X}_2 over the stripes S_1 and S_2 , respectively, are colinear over their whole intersection, the discontinuity manifold $\Sigma_{\frac{\pi}{2}}$.

In fact, as represented at Figure 15a, for \mathbf{F}_1 the slow manifold consists of the straight lines given by $\theta = \theta_1 = -\frac{\pi}{4}$ and $\theta = \theta_1 + \pi = \frac{3\pi}{4}$; over then acts the increasing dynamics $\dot{x} = 1$. Besides that, the first line is repellor and, the second, attractor of the allround dynamics. On the other hand, as represented at Figure 15b, for \mathbf{F}_2 the slow manifold consists of the straight lines given by $\theta = \theta_2 = \frac{\pi}{4}$ and $\theta = \theta_2 + \pi = \frac{5\pi}{4}$; over then acts the decreasing dynamics $\dot{x} = -1$. Besides that, the first line is attractor and, the second, repellor of the surrounding layer dynamics. In other words, the only differences between their dynamics is a π -translation in θ and inverse stability.

This symmetry assures the colinearity of \mathbf{X}_1 and \mathbf{X}_2 over $\Sigma_{\frac{\pi}{2}}$, as represented at Figure 15c. Hence, the final part of Theorem 7.1 is violated and, therefore, this configuration is structurally unstable around $\Sigma_{\frac{\pi}{2}}$, whatever the convex compact set K considered. Geometrically, the instability here comes from the fact that each point of colinearity is associated with a pseudo-singularity of the sliding vector field of the Filippov system $\mathbf{X} = (\mathbf{X}_1, \mathbf{X}_2)$ and, at our configuration we have a continuum of them. This whole continuum of pseudo-singularities can be easily destroyed by perturbing any of associated vector fields. \square

7.2 Affine Dynamics

Let $\mathbf{F} \in \mathcal{A}_3$ be a piecewise smooth vector field with a double discontinuity given by affine vector fields

$$\begin{aligned} \mathbf{F}_i(x, y, z) = & (a_{i1}x + b_{i1}y + c_{i1}z + d_{i1}, \\ & a_{i2}x + b_{i2}y + c_{i2}z + d_{i2}, \\ & a_{i3}x + b_{i3}y + c_{i3}z + d_{i3}), \end{aligned} \quad (37)$$

with $\gamma_i \neq 0$. Remember that, in this case, Theorem 6.1 provides a full description of the fundamental dynamics of (37) and, therefore, as in the previous section, we would like

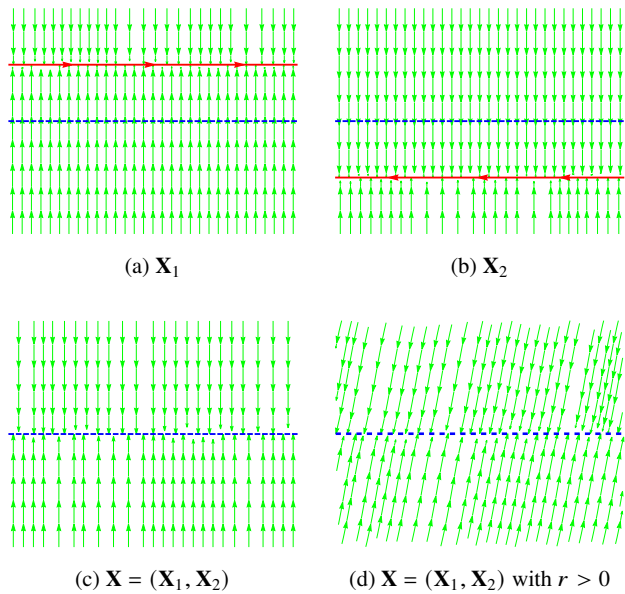


Fig. 15: Dynamics over the stripes $S_1 \cup S_2$ generated by the fields studied at Example 7.1.

to combine it with Proposition 7.2 to derive a semi-local structural stability theorem.

In order to apply this results, given $\Sigma_{\theta_0} \in \tilde{\mathcal{I}}_C$, let $\mathbf{X} = (\mathbf{X}_-, \mathbf{X}_+)$ be the Filippov system induced by (37) in a convex compact set $K \subset C_+ \cup C_-$, where C_+ and C_- are two consecutive stripes meeting at Σ_{θ_0} as represented at Figure 14. According to Theorem 6.1, the following are the possible categories of dynamics for a stripe $S_i \in \{C_+, C_-\}$, which we now analyze against conditions (C.1) — (C.5) of Proposition 7.2 case by case in order to discover those that can possibly generate structural stable systems, i.e., the *candidates*:

1. $a_{i2} \neq 0$:

- (a) $a_{i3} \neq 0$:

The characterizing property of this case is the fact that $\beta_i \neq 0$ and, therefore, the horizontal asymptotes resides inside the stripes, possibly even S_i . As a consequence, there is always a visible part of the slow manifold inside S_i . Hence, if $a_{i1} = 0$ and $d_{i1} = 0$, then we have a continuum of singularities; if $a_{i1} = 0$ and $d_{i1} \neq 0$, then we have a similar bifurcation to that described at Proposition 7.3 when perturbing. Either way, (C.1) is violated. However, if $a_{i1} \neq 0$, then Theorem 4.5 assures the existence of at most one robust singularity \mathbf{P} , always hyperbolic and, therefore, (C.1) and (C.2) validates, since obviously there is no periodic orbits inside S_i . As in the constant case, the α or ω -limit nature of the slow manifold also assures (C.3). For (C.4) and (C.5), observe that the fast dynamics is always transversal and, therefore, we only need

the additional condition $\mathbf{P} \notin \Sigma_{\theta_0}$. Finally, as in the constant case, invoking theorems such as *continuity theorems* and *Thom Transversality Theorem*, we easily conclude the robustness of the properties validated above when perturbing inside \mathcal{A}_3 . Therefore, this case is a *candidate* if, and only if, $a_{i1} \neq 0$ and $\mathbf{P} \notin \Sigma_{\theta_0}$.

(b) $a_{i3} = 0$:

The only difference between this case and the previous is the fact that $\beta_i = 0$ and, therefore, the horizontal asymptotes are exactly at the borders $\theta = 0$ and $\theta = \pi$ of the stripes. However, since we are working inside a convex compact set K , then the same arguments of the previous case apply here.

2. $a_{i2} = 0$:

Finally, the only difference between this case and the previous ($a_{i2} \neq 0$ and $a_{i3} = 0$) is the fact that now the horizontal asymptotes are exactly at the borders $\theta = \pi/2$ and $\theta = 3\pi/2$ of the stripes. Therefore, the same arguments applies.

The analysis of the remaining conditions (C.6) — (C.9) requires the combined dynamics of the stripes C_+ and C_- . Therefore, in order to decide stability, we need to analyze all the combinations of candidates obtained above against these conditions. Generally, it is fairly easy to perform this analysis given a specific combination. However, a translation of these final conditions to parametric ones, although possible, would lead to a relatively large number¹³ of conditions that, worse than that, would carry little to no geometrical meaning. Hence, leaving these final conditions “untranslated” is a better approach and, therefore, the following theorem has been proved:

Theorem 7.2 (Affine Dynamics Stability) *Let $\mathbf{F} \in \mathcal{A}_3$ be given by (37) with $\gamma_i \neq 0$. Given $\Sigma_{\theta_0} \in \tilde{\mathcal{I}}_C$, let $\mathbf{X} = (\mathbf{X}_-, \mathbf{X}_+)$ be the Filippov system induced around Σ_{θ_0} and inside a convex compact set $K \subset C_+ \cup C_-$, where C_+ and C_- are two consecutive stripes meeting at Σ_{θ_0} . Then, \mathbf{F} is (Σ_{θ_0}, K) -semi-local structurally stable in \mathcal{A}_3 if, and only if, \mathbf{X}_+ and \mathbf{X}_- satisfies*

1. $a_{i1} \neq 0$ and $\mathbf{P} \notin \Sigma_{\theta_0}$, where \mathbf{P} is the only singularity of \mathbf{X}_{\pm} ;
2. conditions (C.6) — (C.9) of Proposition 7.2.

Example 7.2 Lets see an example of instability around the discontinuity manifold $\Sigma_0 \in \tilde{\mathcal{I}}_C$ of the cylinder generated by affine vector fields. More precisely, take $\mathbf{F} \in \mathcal{A}_3$ with \mathbf{F}_4 and \mathbf{F}_1 affine vector fields given by (37) such that

$$\mathbf{F}_4 : \begin{bmatrix} a_{41} & d_{41} \\ a_{42} & d_{42} \\ a_{43} & d_{43} \end{bmatrix} = \begin{bmatrix} -1 & 1 \\ 0 & -1 \\ 1 & 0 \end{bmatrix} \quad \text{and} \quad \mathbf{F}_1 : \begin{bmatrix} a_{11} & d_{11} \\ a_{12} & d_{12} \\ a_{13} & d_{13} \end{bmatrix} = \begin{bmatrix} 1 & -1 \\ 0 & 1 \\ 1 & 0 \end{bmatrix},$$

whose dynamics over the stripes $S_4 \cup S_1$, represented at Figure 16 below, can be determined as in Example 6.1 using Theorem 6.1.

Regarding \mathbf{F}_4 , since $a_{42} = 0$ and $\gamma_4 = -1 < 0$, then Theorem 6.1 tells us that the slow manifold is a decreasing arctangent with horizontal asymptotes $\theta = -\pi/2$ and $\theta = \pi/2$, as represented at Figure 16a. This manifold crosses the line $\theta = \theta_0 = 0$ at $x \in \mathbb{R}$ such that

$$\begin{aligned} 0 = \theta_0 = \theta_4(x) &= \arctan\left(\frac{a_{43}x + d_{43}}{d_{42}}\right) = \\ &= \arctan(-x) \Leftrightarrow x = 0, \end{aligned}$$

i.e., at the point $\mathbf{Q}_4 = (0, 0)$. Besides that, over the slow manifold acts the dynamics $\dot{x} = -x+1$ whose only singularity at the point

$$\mathbf{P}_4 = (\delta_4, \theta_4(\delta_4)) = (1, \arctan(-1)) = \left(1, -\frac{\pi}{4}\right),$$

is stable, since $a_{41} < 0$. Even more, since $a_{42} = 0$ and $d_{42} < 0$ then, according to Table 3, the slow manifold repels the layer dynamics around. Therefore, remembering of Theorem 4.5 we conclude that \mathbf{P}_4 , as a singularity of \mathbf{X}_4 , is a hyperbolic *saddle*.

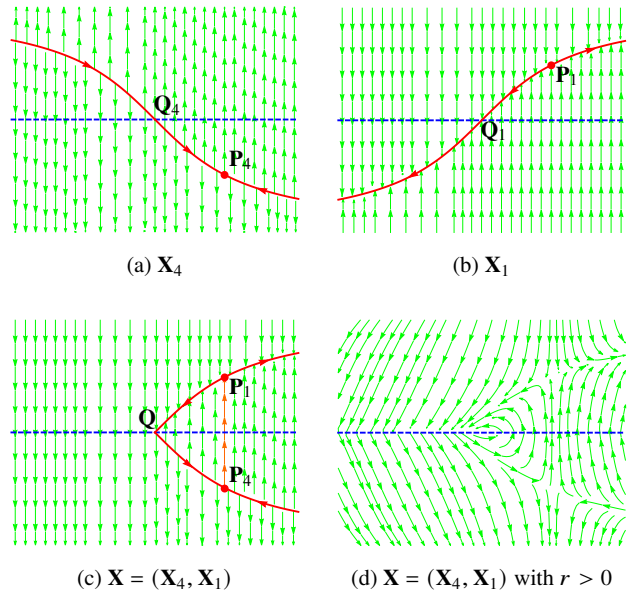


Fig. 16: Dynamics over the stripes $S_4 \cup S_1$ generated by the fields studied at Example 7.2.

¹³ More specifically, Theorem 6.1 give us a normal form with 8 possible dynamics for each stripe. Combining them 2 by 2 (with repetition) leave us with 36 combinations. Even if half of the combinations lead to a repeating condition, we would still be left with 18 conditions!

On the other hand, regarding \mathbf{F}_1 , since $a_{12} = 0$ and $\gamma_1 = 1 > 0$, then Theorem 6.1 tells us that the slow manifold is a decreasing arctangent with horizontal asymptotes $\theta = -\pi/2$ and $\theta = \pi/2$, as represented at Figure 16b. This manifold crosses the line $\theta = \theta_0 = 0$ at $x \in \mathbb{R}$ such that

$$\begin{aligned} 0 = \theta_0 = \theta_1(x) &= \arctan\left(\frac{a_{13}x + d_{13}}{d_{12}}\right) \\ &= \arctan(x) \Leftrightarrow x = 0, \end{aligned}$$

i.e., also at the point $\mathbf{Q}_1 = (0, 0)$. Besides that, over the slow manifold acts the dynamics $\dot{x} = x - 1$ whose only singularity at the point

$$\mathbf{P}_1 = (\delta_1, \theta_1(\delta_1)) = (1, \arctan(1)) = \left(1, \frac{\pi}{4}\right),$$

is unstable, since $a_{11} > 0$. Even more, since $a_{12} = 0$ and $d_{12} > 0$ then, according to Table 3, the slow manifold attracts the layer dynamics around. Therefore, remembering Theorem 4.5 we conclude that \mathbf{P}_1 , as a singularity of \mathbf{X}_1 , is also a hyperbolic *saddle*.

Hence, as represented at Figure 16c, since $\mathbf{Q}_4 = \mathbf{Q}_1$ with \mathbf{P}_4 and \mathbf{P}_1 hyperbolic saddles, then the Filippov system $\mathbf{X} = (\mathbf{X}_4, \mathbf{X}_1)$ has a separatrix-connection and, therefore, it violates condition (C.8) of Proposition 7.2, whatever the convex compact set K considered. In other words, according to Theorem 7.2, this configuration is structurally unstable around the discontinuity manifold Σ_0 .

Finally, we observe that, as represented at Figure 16c, there is actually two separatrix-connections between the saddles \mathbf{P}_4 and \mathbf{P}_1 . These connections enclose a *rotating region*, represented at Figure 16d. \square

8 Conclusion

In this work, we tackled the problems stated at Section 3: given \mathbf{F} with a double discontinuity (two switches) as switching manifold, can we define Filippov-like dynamics over the singular part, i.e., the intersection Σ_x ? How do these dynamics generally behave there? Specifically, we leveraged *Buzzi's* blow-up methodology to approach these problems, resulting initially in the Fundamental Lemma 4.1, which induces the so-called *fundamental dynamics*: a (regular) discontinuous slow-fast dynamics happening over a cylinder representing Σ_x after the blow-up. Many qualitative properties were derived for the general non-linear case, as long as one of the so-called *fundamental hypotheses* was satisfied.

Especially, when \mathbf{F} is composed of constant or affine vector fields, we were able to fully describe the qualitative aspects of the fundamental dynamics as presented in Theorem 5.1 and Theorem 6.1, respectively. Once we had this knowledge, [7, 22] inspired us to look after the semi-local

structural stability of the fundamental dynamics, resulting in Theorem 7.1 and Theorem 7.2, which characterize stability through a set of simple algebraical and geometrical conditions.

To the best of our knowledge, none of the other methodologies (*Jeffrey's* and *Dieci's*) discussed in Section 1 were able to deliver similar results, expressing then the effectiveness and practicality of *Buzzi's* blow-up based methodology as presented and improved here. However, we acknowledge the beauty of *Jeffrey's* canopy based methodology, which directly extends the Filippov dynamics to the singular part of the switching manifold through convex combinations. In fact, we conjecture and look forward to prove the equivalence of these methodologies, then unifying its strengths.

Howsoever, on the applicability of these methodologies, we expand the remark in section 8.1 of [26, p. 1102] by Mike Jeffrey as follows:

“If one is able to find physical laws for the dynamics on \mathcal{D} , then these supersede the discontinuous model (. . .), and whether these agree with the ~~canopy and dummy dynamics model~~ is open for experimenters of various disciplines to put to the test.”

Nature has the final word.

Declarations

Funding The first author was financed in part by the Coordenação de Aperfeiçoamento de Pessoal de Nível Superior — Brasil (CAPES) — Finance Code 001. The second author was partially supported by FAPESP grants 2018/03338–6 and 2018/13481–0.

Conflict of interest The authors declare that they have no conflict of interest.

Availability of data and material Not applicable.

Code availability Not applicable.

References

1. Amador, J.A., Olivar, G., Angulo, F.: Smooth and Filippov models of sustainable development: bifurcations and numerical computations. *Differential Equations and Dynamical Systems* **21**(1-2), 173–184 (2013). doi:10.1007/s12591-012-0138-2
2. Arrowsmith, D.K., Place, C.M.: *An Introduction to Dynamical Systems*. Cambridge University Press (1990)
3. Barry, A.M., Widiasih, E., McGehee, R.: Nonsmooth frameworks for an extended Budyko model. *Discrete and Continuous Dynamical Systems - B* **22**(6), 2447–2463 (2017). doi:10.3934/dcdsb.2017125

4. di Bernardo, M., Garefalo, F., Glielmo, L., Vasca, F.: Switchings, bifurcations, and chaos in DC/DC converters. *IEEE Transactions on Circuits and Systems I* **45**(2), 133–141 (1998). doi:10.1109/81.661675
5. Bernardo, M.D., Johansson, K.H., Vasca, F.: Self-Oscillations and Sliding in Relay Feedback Systems: Symmetry and Bifurcations. *International Journal of Bifurcation and Chaos* **11**(4), 1121–1140 (2001). doi:10.1142/S0218127401002584
6. Brogliato, B.: *Nonsmooth Mechanics: Models, Dynamics and Control*, 2 edn. Springer-Verlag London (1999). doi:10.1007/978-1-4471-0557-2
7. Broucke, M.E., Pugh, C., Simic, S.N.: Structural Stability of Piecewise Smooth Systems. *Computational and Applied Mathematics* **20**(1-2), 51–89 (2001)
8. Buzzi, C.A., da Silva, P.R., Teixeira, M.A.: Slow-fast systems on algebraic varieties bordering piecewise-smooth dynamical systems. *Bulletin des Sciences Mathématiques* **136**(4), 444–462 (2012). doi:10.1016/j.bulsci.2011.06.001
9. de Carvalho, T., Novaes, D.D., Gonçalves, L.F.: Sliding Shilnikov connection in Filippov-type predator-prey model. *Nonlinear Dynamics* **100**(3), 2973–2987 (2020). doi:10.1007/s11071-020-05672-w
10. Cristiano, R., Pagano, D.J., Freire, E., Ponce, E.: Revisiting the Teixeira singularity bifurcation analysis: application to the control of power converters. *Int. J. Bifurcation Chaos* **28**(9), 31 (2018). doi:10.1142/S0218127418501067
11. Dieci, L.: Sliding motion on the intersection of two manifolds: Spirally attractive case. *Communications in Nonlinear Science and Numerical Simulation* **26**(1), 65–74 (2015). doi:10.1016/j.cnsns.2015.02.002
12. Dieci, L., Difonzo, F.: A comparison of Filippov sliding vector fields in codimension 2. *Journal of Computational and Applied Mathematics* **262**, 161–179 (2014). doi:10.1016/j.cam.2013.10.055
13. Dieci, L., Elia, C.: Piecewise smooth systems near a co-dimension 2 discontinuity manifold: Can one say what should happen? *Discrete and Continuous Dynamical Systems - S* **9**(4), 1039–1068 (2016). doi:10.3934/dcdss.2016041
14. Dieci, L., Elia, C., Lopez, L.: A Filippov sliding vector field on an attracting co-dimension 2 discontinuity surface, and a limited loss-of-attractivity analysis. *Journal of Differential Equations* **254**(4), 1800–1832 (2013). doi:10.1016/j.jde.2012.11.007
15. Dieci, L., Elia, C., Lopez, L.: Sharp sufficient attractivity conditions for sliding on a co-dimension 2 discontinuity surface. *Mathematics and Computers in Simulation* **110**, 3–14 (2015). doi:10.1016/j.matcom.2013.12.005
16. Dieci, L., Elia, C., Lopez, L.: Uniqueness of Filippov sliding vector field on the intersection of two surfaces in \mathbb{R}^3 and implications for stability of periodic orbits. *Journal of Nonlinear Science* **25**(6), 1453–1471 (2015). doi:10.1007/s00332-015-9265-6
17. DIECI, L., LOPEZ, L.: Sliding motion in Filippov differential systems: theoretical results and a computational approach. *SIAM Journal on Numerical Analysis* **47**(3), 2023–2051 (2009). doi:10.1137/080724599
18. Dieci, L., Lopez, L.: Sliding motion on discontinuity surfaces of high co-dimension. A construction for selecting a Filippov vector field. *Numerische Mathematik* **117**(4), 779–811 (2011). doi:10.1007/s00211-011-0365-4
19. Fenichel, N.: Geometric singular perturbation theory for ordinary differential equations. *Journal of Differential Equations* **31**(1), 53–98 (1979). doi:10.1016/0022-0396(79)90152-9
20. Filippov, A.F.: *Differential Equations with Discontinuous Right-hand Sides*. 18. Springer Netherlands (1988). doi:10.1007/978-94-015-7793-9
21. Glendinning, P., Jeffrey, M.R.: *An Introduction to Piecewise Smooth Dynamics*. *Advanced Courses in Mathematics - CRM Barcelona*. Birkhäuser Basel (2019). doi:10.1007/978-3-030-23689-2
22. Gomide, O.M.L., Teixeira, M.A.: On structural stability of 3D Filippov systems. *Mathematische Zeitschrift* **294**(1-2), 419–449 (2020). doi:10.1007/s00209-019-02252-6
23. Guardia, M., Seara, T.M., Teixeira, M.A.: Generic bifurcations of low codimension of planar Filippov systems. *Journal of Differential equations* **250**(4), 1967–2023 (2011). doi:10.1016/j.jde.2010.11.016
24. Gutierrez, C., Sotomayor, J.: Stable Vector Fields on Manifolds with Simple Singularities. *Proceedings of the London Mathematical Society* **45**(1), 97–112 (1982). doi:10.1112/plms/s3-45.1.97
25. Hinrichs, N., Oestreich, M., Popp, K.: On the Modelling of Friction Oscillators. *Journal of Sound Vibration* **216**(3), 435–459 (1998). doi:10.1006/jsvi.1998.1736
26. Jeffrey, M.R.: Dynamics at a switching intersection: Hierarchy, isonomy, and multiple sliding. *SIAM Journal on Applied Dynamical Systems* **13**(3), 1082–1105 (2014). doi:10.1137/13093368X
27. Jeffrey, M.R.: *Hidden Dynamics: The mathematics of switches, decisions, and other discontinuous behaviour*. Springer (2018). doi:10.1007/978-3-030-02107-8
28. Jeffrey, M.R.: *Modeling with Nonsmooth Dynamics*. Springer (2020). doi:10.1007/978-3-030-35987-4
29. Kaklamanos, P., Kristiansen, K.U.: Regularization and geometry of piecewise smooth systems with intersecting discontinuity sets. *SIAM Journal on Applied Dynamical Systems* **18**(3), 1225–1264 (2019). doi:10.1137/18m1214470
30. Katok, A., Hasselblatt, B.: *Introduction to the Modern Theory of Dynamical Systems*. *Encyclopedia of Mathematics and its Applications*. Cambridge University Press (1997)
31. Kowalczyk, P., Piironen, P.T.: Two-parameter sliding bifurcations of periodic solutions in a dry-friction oscillator. *Physica D* **237**(8), 1053–1073 (2008). doi:10.1016/j.physd.2007.12.007
32. Leifeld, J.: Non-smooth homoclinic bifurcation in a conceptual climate model. *European Journal of Applied Mathematics* **29**(5), 891–904 (2018). doi:10.1017/S0956792518000153
33. Llibre, J., da Silva, P.R., Teixeira, M.A.: Sliding vector fields for non-smooth dynamical systems having intersecting switching manifolds. *Nonlinearity* **28**(2), 493–507 (2015). doi:10.1088/0951-7715/28/2/493
34. Novaes, D.D.: Regularization and minimal sets for non-smooth dynamical systems. Ph.D. thesis, Universidade Estadual de Campinas (2015). URL <http://repositorio.unicamp.br/jspui/handle/REPOSIP/305995>
35. Palis, J., de Melo, W.: *Geometric Theory of Dynamical Systems*. Springer-Verlag New York (1982)
36. Panazzolo, D., da Silva, P.R.: Regularization of discontinuous foliations: Blowing up and sliding conditions via Fenichel theory. *Journal of Differential Equations* **263**(12), 8362–8390 (2017). doi:10.1016/j.jde.2017.08.042
37. Piltz, S.H., Porter, M.A., Maini, P.K.: Prey switching with a linear preference trade-off. *SIAM Journal on Applied Dynamical Systems* **13**(2), 658–682 (2014). doi:10.1137/130910920
38. Prokopiou, S.A., Byrne, H.M., Jeffrey, M.R., Robinson, R.S., Mann, G.E., Owen, M.R.: Mathematical analysis of a model for the growth of the bovine corpus luteum. *Journal of Mathematical Biology* **69**(6-7), 1515–1546 (2014). doi:10.1007/s00285-013-0722-2
39. da Silva, G.T., Martins, R.M.: Dynamics and Stability of Non-Smooth Dynamical Systems with Two Switches. arXiv:2009.08971 (2021). URL <https://arxiv.org/abs/2009.08971>
40. Sotomayor, J., Teixeira, M.A.: Regularization of discontinuous vector fields. *International Conference on Differential Equations* (1996)
41. Spraker, J.S.: A Comparison of the Carathéodory and Filippov Solution Sets. *Journal of Mathematical Analysis and Applications* **198**(2), 571–580 (1996). doi:10.1006/jmaa.1996.0099

42. Teixeira, M.A.: Stability conditions for discontinuous vector fields. *Journal of Differential Equations* **88**(1), 15–29 (1990). doi:10.1016/0022-0396(90)90106-Y
43. Teixeira, M.A., da Silva, P.R.: Regularization and singular perturbation techniques for non-smooth systems. *Physica D: Nonlinear Phenomena* **241**(22), 1948–1955 (2012). doi:10.1016/j.physd.2011.06.022
44. Utkin, V.I.: *Sliding Modes in Control and Optimization*. Springer-Verlag (1992). doi:10.1007/978-3-642-84379-2
45. Valencia-Calvo, J., Olivar-Tost, G., Morcillo-Bastidas, J.D., Franco-Cardona, C.J., Dyner, I.: Non-Smooth Dynamics in Energy Market Models: A Complex Approximation From System Dynamics and Dynamical Systems Approach. *IEEE Access* **8**, 128877–128896 (2020). doi:10.1109/ACCESS.2020.3008709
46. Wang, A., Xiao, Y., Zhu, H.: Dynamics of a Filippov epidemic model with limited hospital beds. *Mathematical Biosciences and Engineering* **15**(3), 739–764 (2018). doi:10.3934/mbe.2018033
47. Wang, B., Xu, J., Wai, R., Cao, B.: Adaptive Sliding-Mode With Hysteresis Control Strategy for Simple Multimode Hybrid Energy Storage System in Electric Vehicles. *IEEE Transactions on Industrial Electronics* **64**(2), 1404–1414 (2017). doi:10.1109/TIE.2016.2618778
48. Webber, S., Jeffrey, M.R.: Two-fold singularities in nonsmooth dynamics—Higher dimensional analogs. *Chaos* **30**(9), 093142 (2020). doi:10.1063/5.0002144
49. Weinan, E.: A Proposal on Machine Learning via Dynamical Systems. *Communications in Mathematics and Statistics* **5**(1), 1–11 (2017). doi:10.1007/s40304-017-0103-z
50. Wojewoda, J., Stefański, A., Wiercigroch, M., Kapitaniak, T.: Hysteretic effects of dry friction: Modelling and experimental studies. *Philos. Trans. R. Soc. A* **366**(1866), 747–765 (2008). doi:10.1098/rsta.2007.2125
51. Zhang, W., Ge, S.S.: A global implicit function theorem without initial point and its applications to control of non-affine systems of high dimensions. *Journal of Mathematical Analysis and Applications* **313**(1), 251–261 (2006). doi:10.1016/j.jmaa.2005.08.072